BERKELEY LAB
Bringing Science Solutions to the World

U.S. DEPARTMENT OF ENERGY
Office of Science

Uni-layer magnets

J. L. Rudeiros Fernandez, P. Ferracin

Table of contents

1. Introduction

Context – US Magnet Development Program: Towards very high-field magnets

Hybrid LTS-HTS magnets

LBNL Hybrid Test (2023)

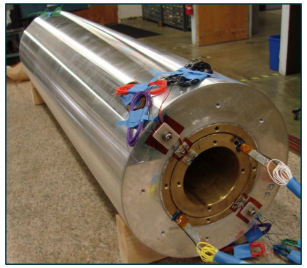

CCT5 as
Nb_3Sn outsert
8-9 T in 90 mm
aperture

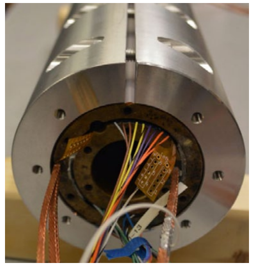

Bin5 as
Nb_3Sn insert
1-2 T in 30 mm
aperture

In development

Nb_3Sn Outserts

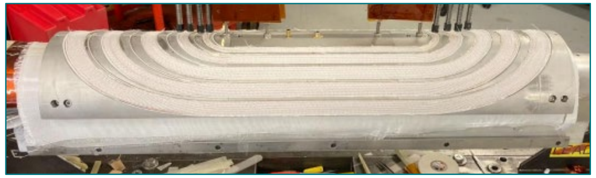

FNAL, SMCT
120 mm aperture (11-12 T)

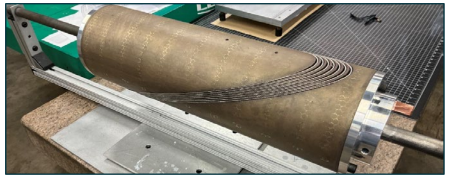

LBNL, CCT6
120 mm aperture (11-12 T)

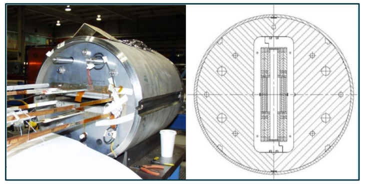

BNL, CC
(10 T)

HTS Inserts

LBNL, REBCO CORC CCT (5 T)

FNAL, REBCO CORC COMB (~5 T)

BNL, REBCO CORC CC insert

FNAL Bi2212 SMCT (~3 T)

LBNL, Bi2212 CCT (3-5 T)

Towards 20 T hybrid accelerator magnets

Ferracin, P., et al. "Conceptual design of 20 T hybrid accelerator dipole magnets." *IEEE Transactions on Applied Superconductivity* (2023).

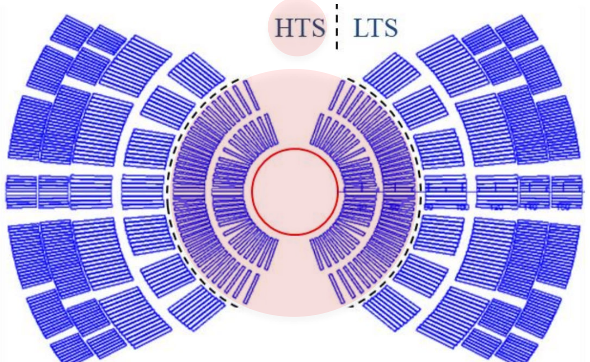

Due to their intrinsic properties and cost, HTS conductors are more effectively used in the innermost layers.

1. Introduction

Context – US MDP

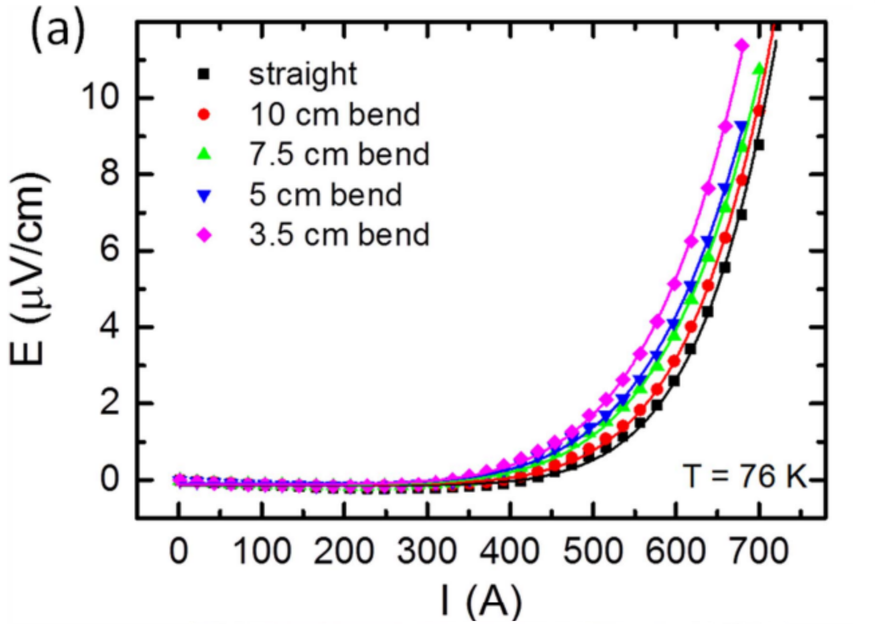

Weiss, Jeremy D., et al. "Introduction of CORC® wires: highly flexible, round high-temperature superconducting wires for magnet and power transmission applications." *Superconductor science and technology* 30.1 (2016): 014002.

A few examples of HTS insert magnet concepts

CORC

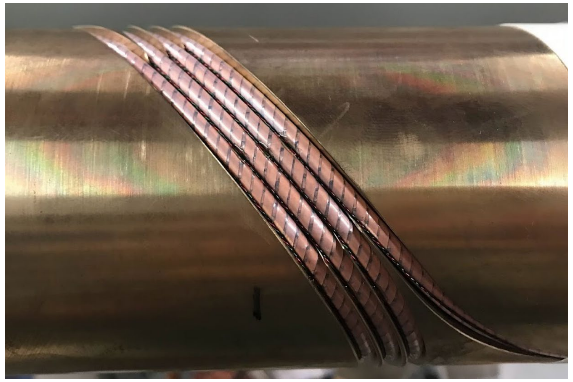

X. Wang (LBNL)

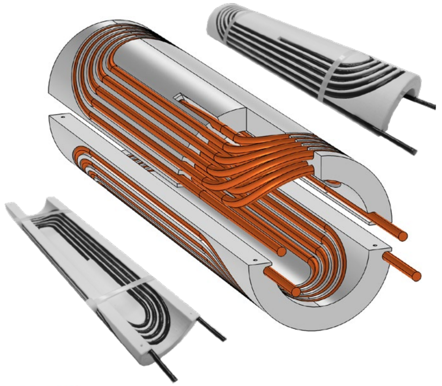

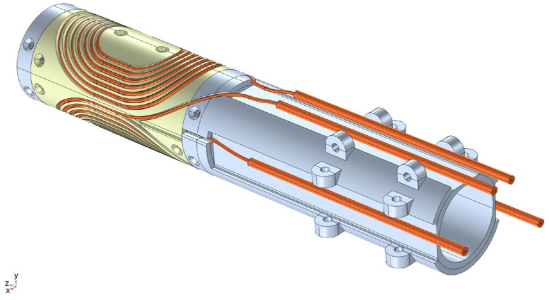

V. Kashikhin (Fermilab)

Bi2212

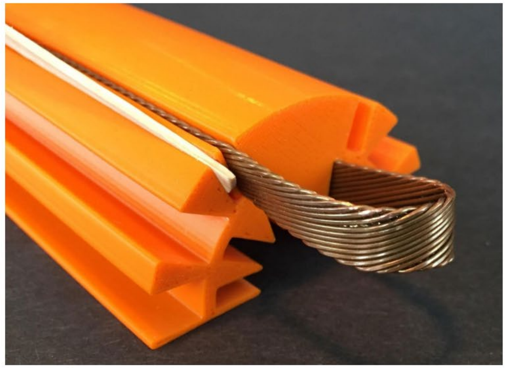

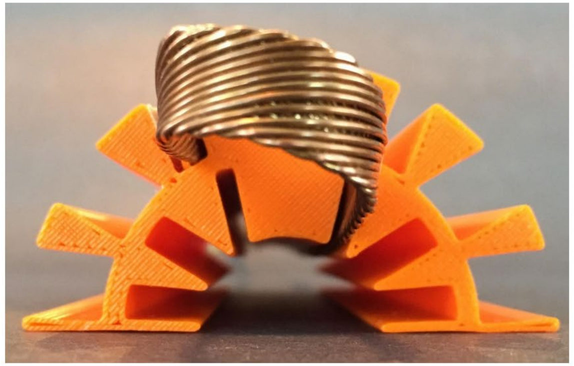

A. Zlobin (Fermilab)

1. Introduction

Key challenges in the performance and cost of future high-field superconducting magnets:

- Magnet design's ability to deal with high Lorentz forces and resulting strain-stress in the strain-sensitive conductor (i.e. **stress management structures**).
- **Efficient** use of the conductor to create a certain magnetic field (i.e. required length of conductor for an equivalent integrated field along the beam path). In terms of efficiency, the ability to implement "grading" is also crucial.
- Magnet design's that enables the **effective use of HTS** superconductors (i.e. magnet designs that could leverage all the potential of HTS superconductors without subjecting it to degradation due to required geometrical or manufacturing conditions).
- **Easiness**, **scalability**, and **cost-effective** manufacturing of the coil and magnet.

Table of contents

2. Uni-layer magnets

A few words on field-quality

$$C_n = B_n + iA_n$$

$$\mathbf{B}(z) = \sum_{n=1}^{\infty} C_n \left(\frac{z}{R_{ref}} \right)^{n-1} \quad \text{with} \quad z \in D$$

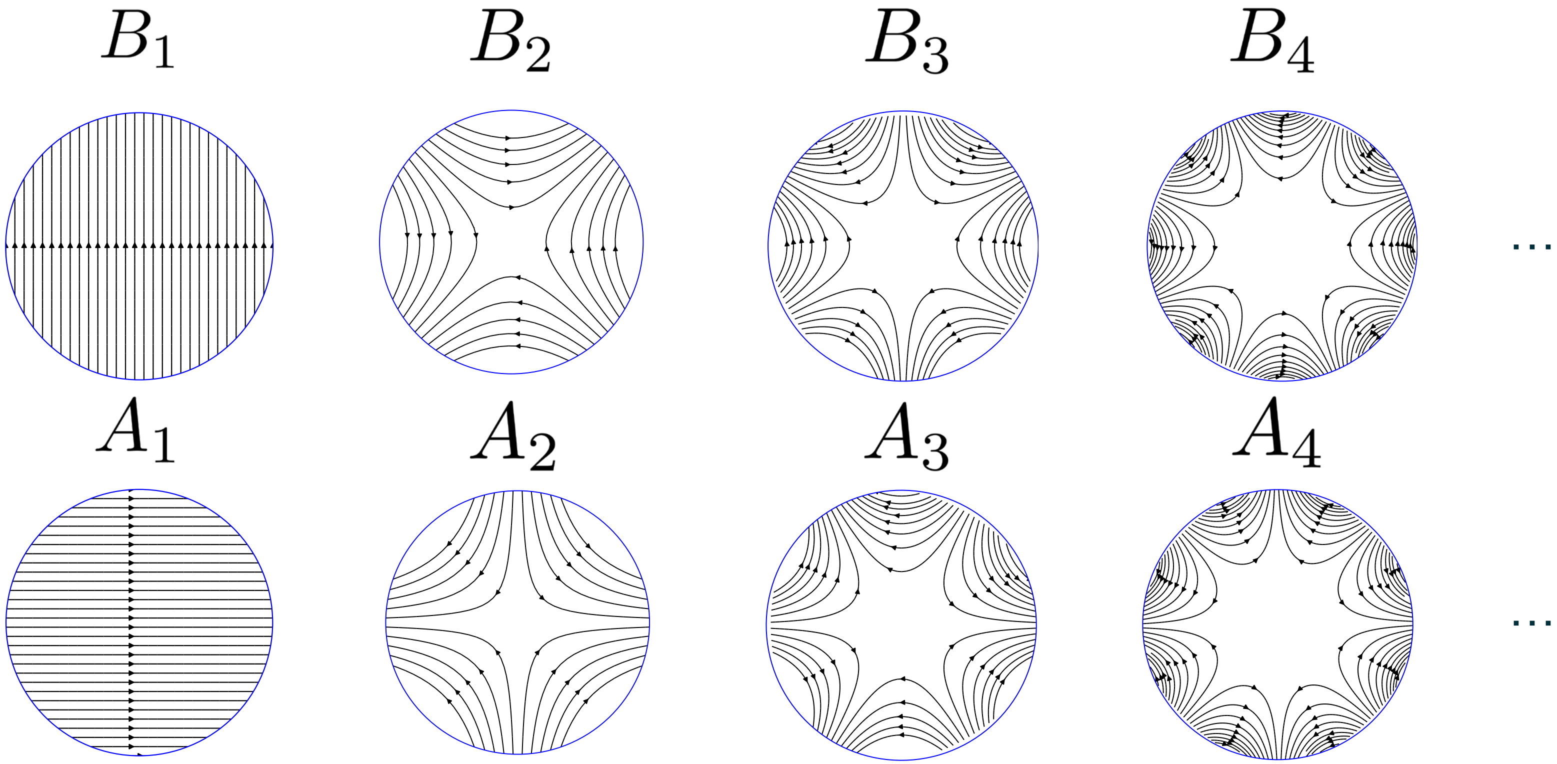

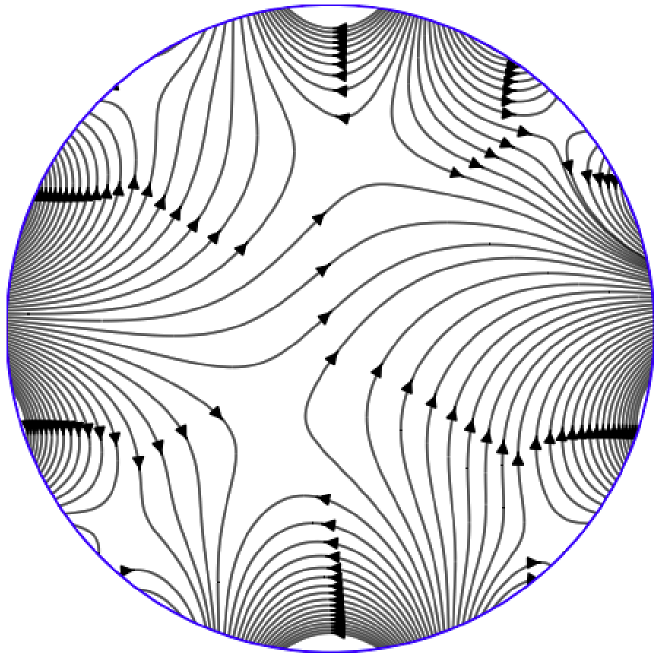

2. Uni-layer magnets

A few words on field-quality

$$\mathbf{B}(z) = \sum_{n=1}^{\infty} C_{n,total} \left(\frac{z}{R_{ref}} \right)^{n-1}$$

$$C_{n,total} = -\frac{\mu_0 R_{ref}^{n-1}}{2\pi} \sum_{j=1}^{m} \frac{I_j}{\rho_j^n} e^{-in\theta_j}$$

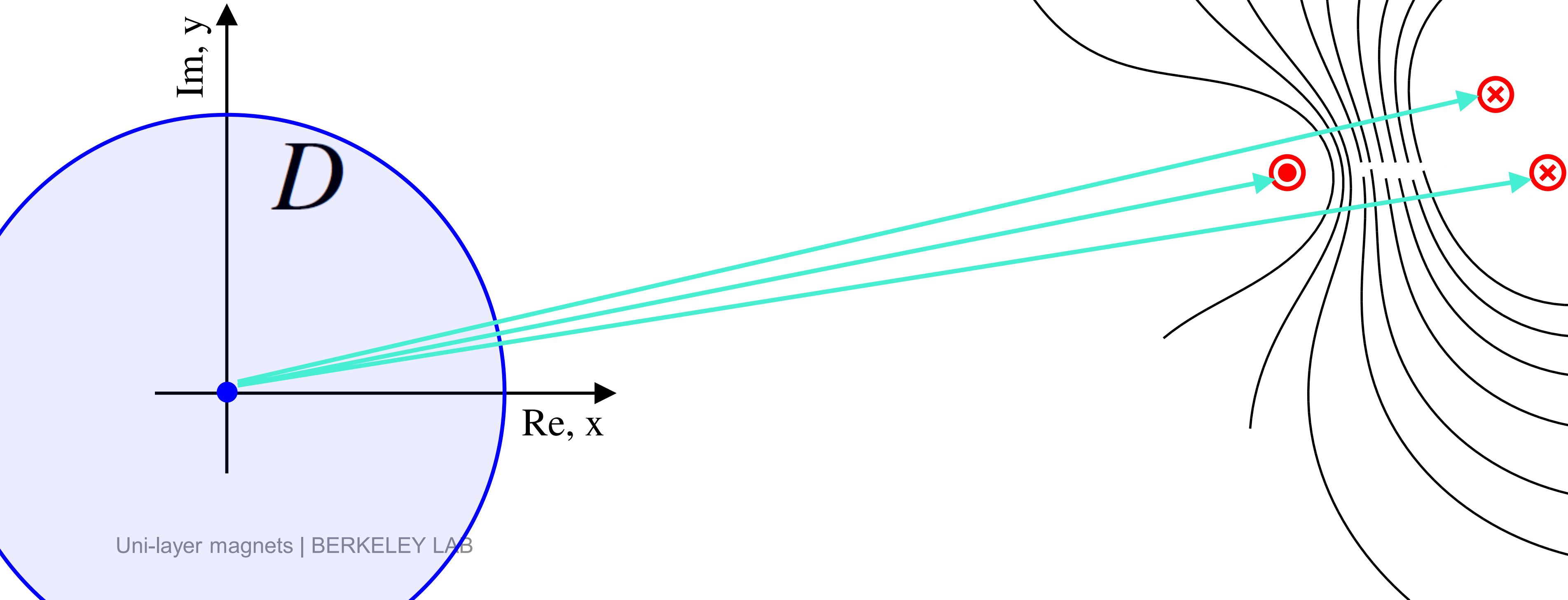

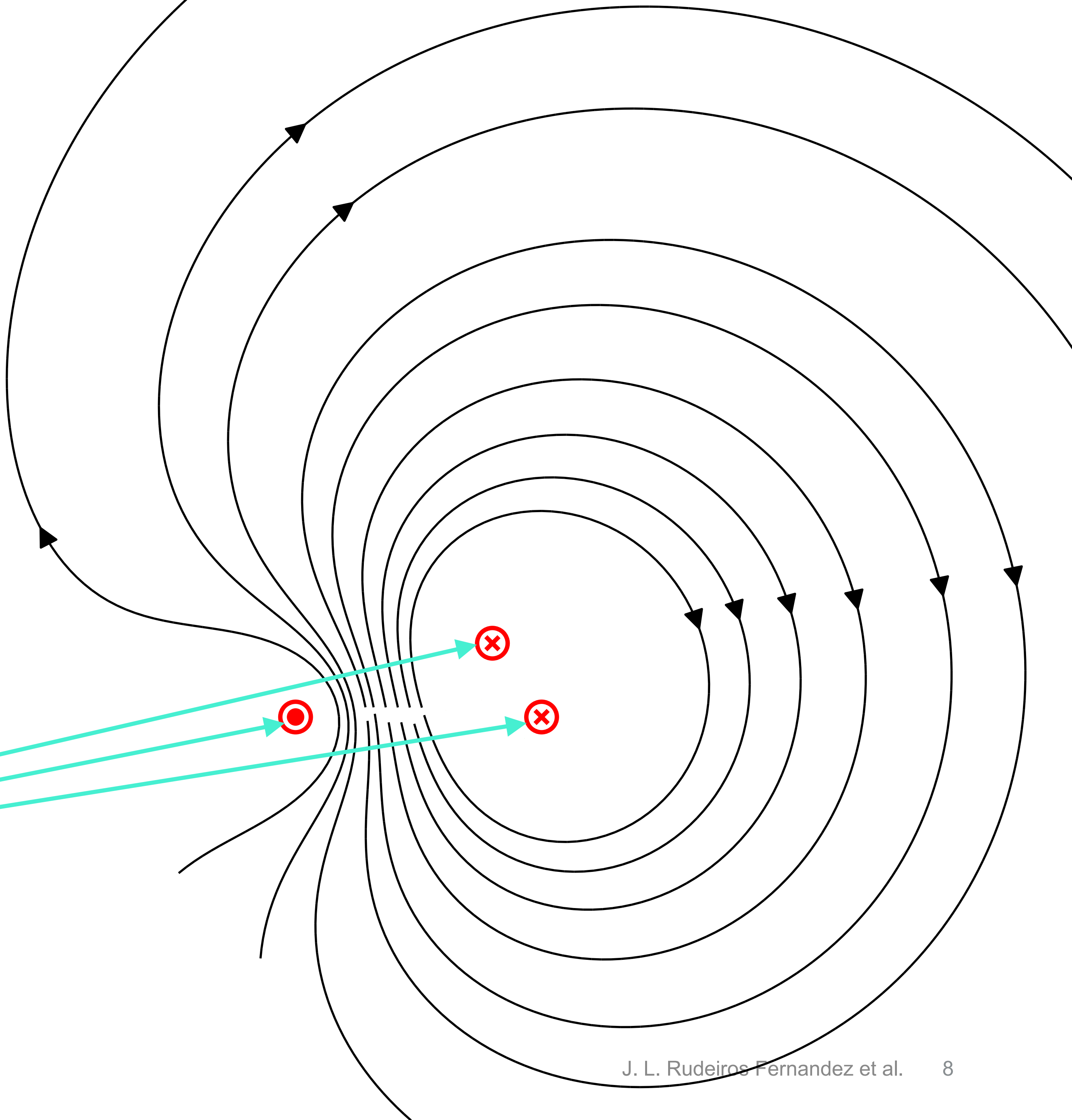

2. Uni-layer magnets

A special case of a system of infinitely long current lines

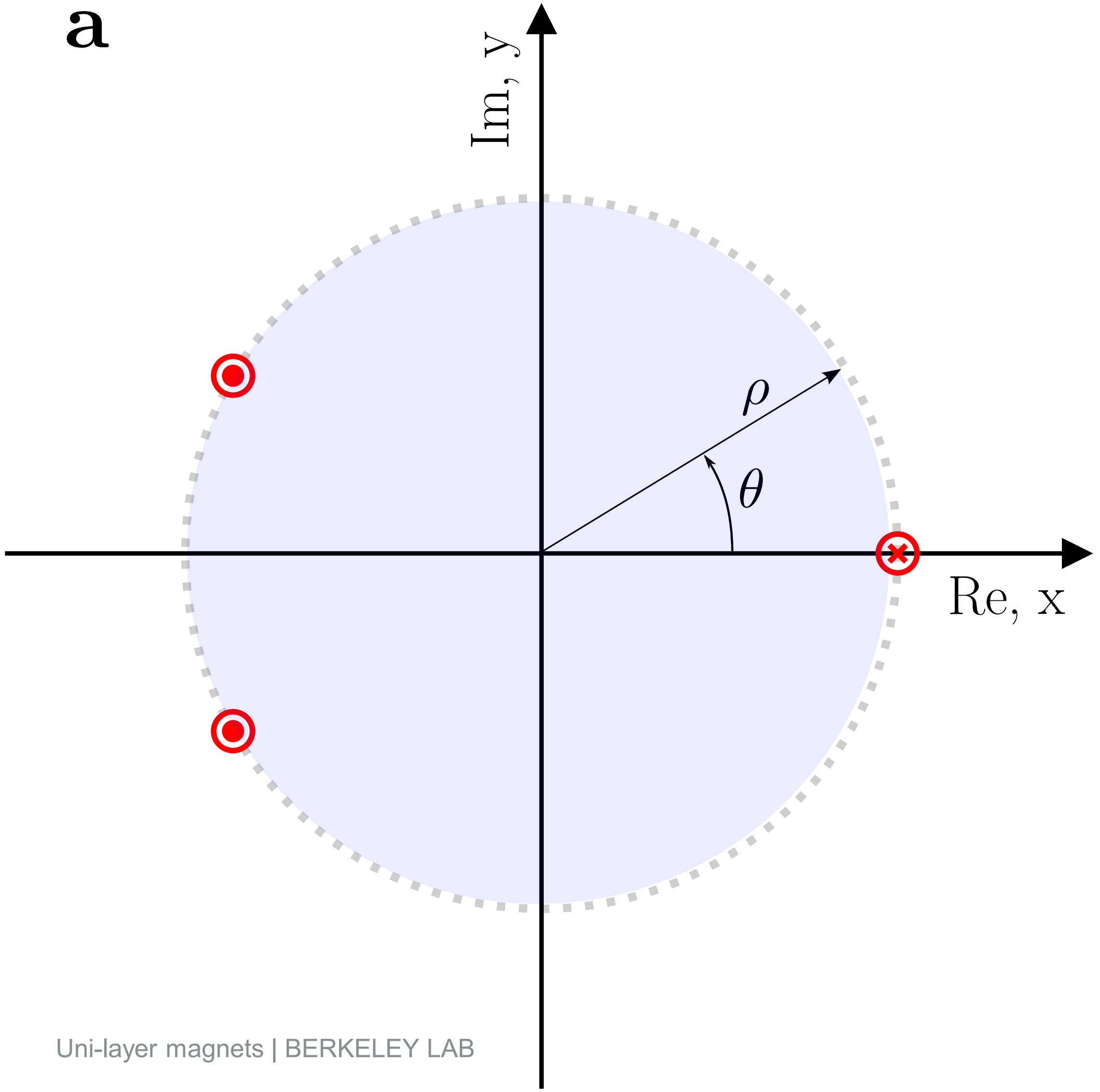

$$\mathbf{B}(z) = \sum_{n=1}^{\infty} C_{n,total} \left(\frac{z}{R_{ref}} \right)^{n-1}$$

$$C_{n,total} = -\frac{\mu_0 R_{ref}^{n-1}}{2\pi} \sum_{j=1}^{m} \frac{I_j}{\rho_j^n} e^{-in\theta_j}$$

$$C_{n,total} = -\frac{\mu_0 I}{2\pi} \frac{R_{ref}^{n-1}}{\rho^n} \sum_{j=1}^{m} s_j e^{-in\theta_j}$$

$$C_{n,t} = \frac{\mu_0 I}{2\pi} \frac{R_{ref}^{n-1}}{\rho^n} \left(-1 + 2\cos\left(n\theta_t\right)\right)$$

2. Uni-layer magnets

Definition

An idealized **Uni-layer** magnet can be defined as a magnet that generates a **B** field within a straight region of space by a system of current lines, all parallel to the *z-axis* (along the straight section of the magnet) of a Cartesian coordinate system (i.e. perpendicular to the *xy-plane*), that lay within a single continuous surface, and that are connected by a single continuous path that does not cross itself.

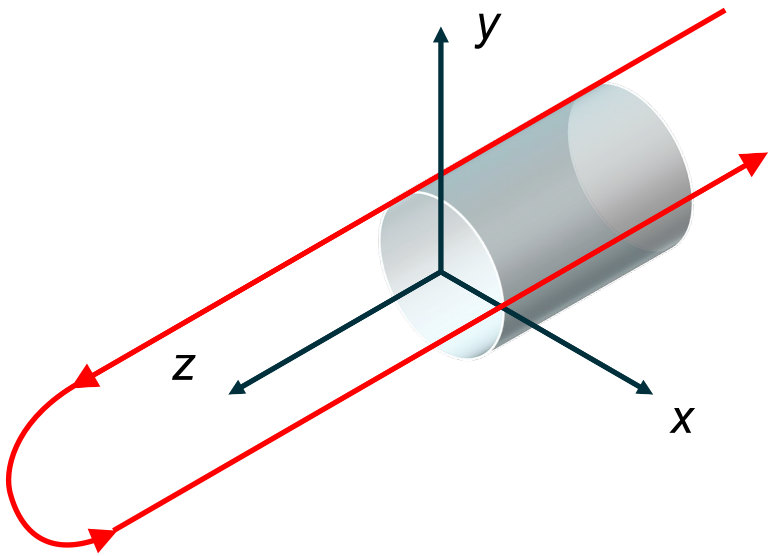

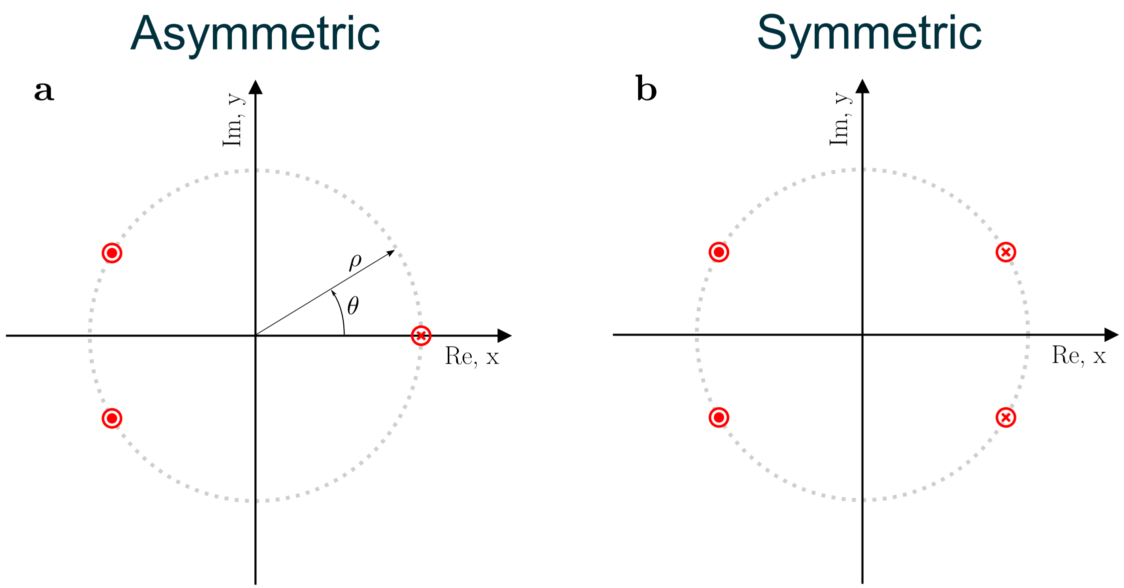

2. Uni-layer magnets

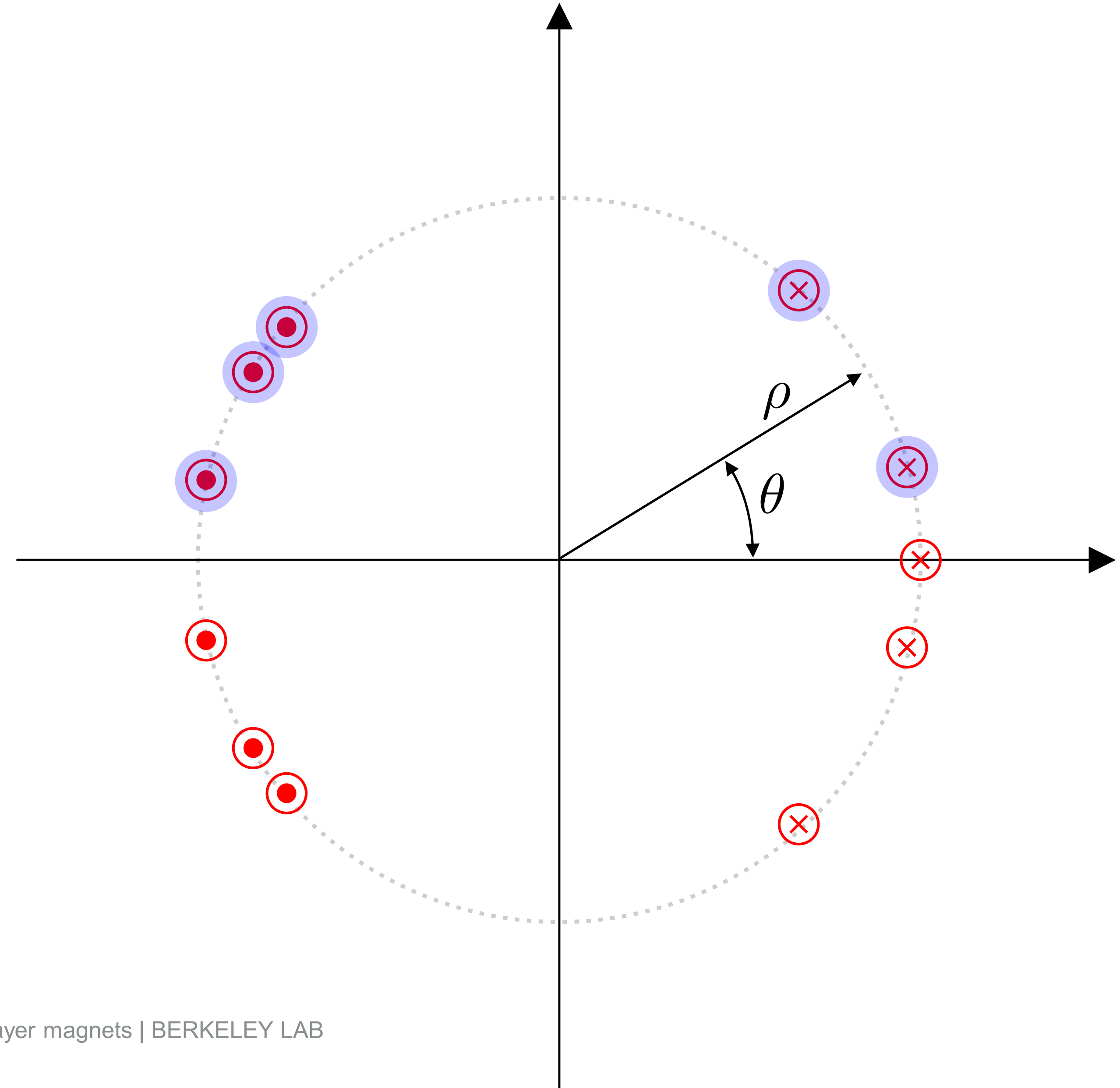

$$\theta = \{\theta_1, \theta_2, \dots \theta_m\}$$

$$\rho = \{\rho_1, \rho_2, \dots \rho_m\}$$

$$I = \{I_1, I_2, \dots I_m\}$$

2. Uni-layer magnets

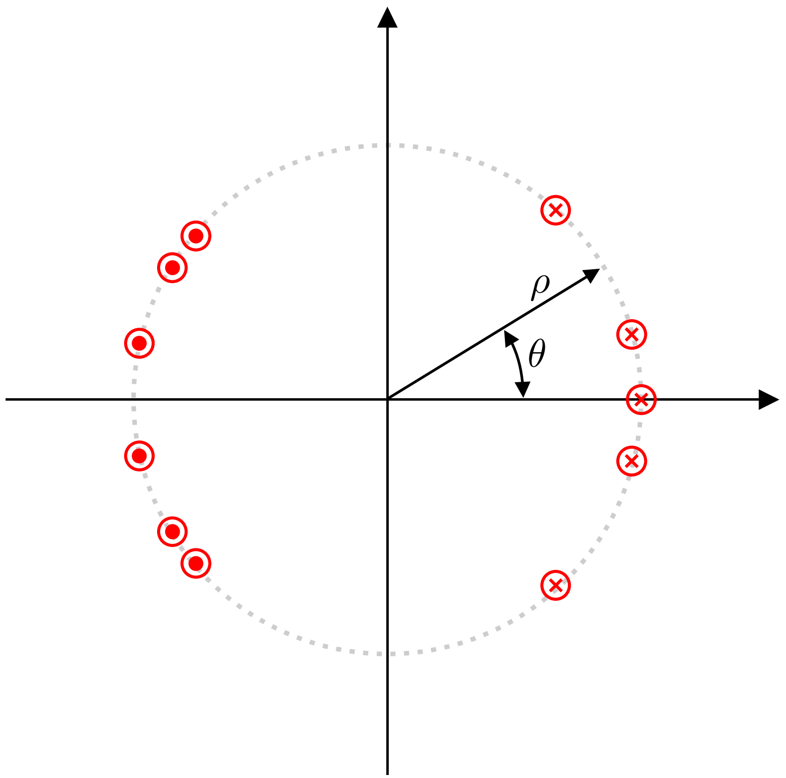

$$\theta = \{\theta_1, \theta_2, \ldots \theta_m\}$$

$$\rho = \{\rho_1, \rho_2, \ldots \rho_m\}$$

$$I = \{I_1, I_2, \ldots I_m\}$$

Harmonic of interest: **B₁**

$$C_{n,total} = -\frac{\mu_0 I}{2\pi} \frac{R_{ref}^{n-1}}{\rho^n} \sum_{j=1}^{m} s_j e^{-in\theta_j}$$

$$-\sum_{j=1}^{m_{opt}} \cos\theta_j + \sum_{j=m_{opt}+1}^{m_r} \cos\theta_j$$

Geometrical constraint: Minimum distance between conductors

$$\min\{\|\theta_j - \theta_{j+1}\|\} - \theta_{min} \geq 0, \quad j = 1, \ldots, m_r - 1$$

Geometrical constraint: *Left-Right* position

$$\theta_{min} \leq \theta_j \leq \frac{\pi}{2}, \quad j = 1, \ldots, m_{opt}$$

$$\frac{\pi}{2} \leq \theta_j \leq \pi, \quad j = m_{opt} + 1, \ldots, m_r$$

Harmonics to be cancelled

$$-1 + 2\left(-\sum_{j=1}^{m_{opt}} \cos n\theta_j + \sum_{j=m_{opt}+1}^{m_r} \cos n\theta_j\right) = 0, \quad n = 1, \ldots, n_0$$

2. Uni-layer magnets

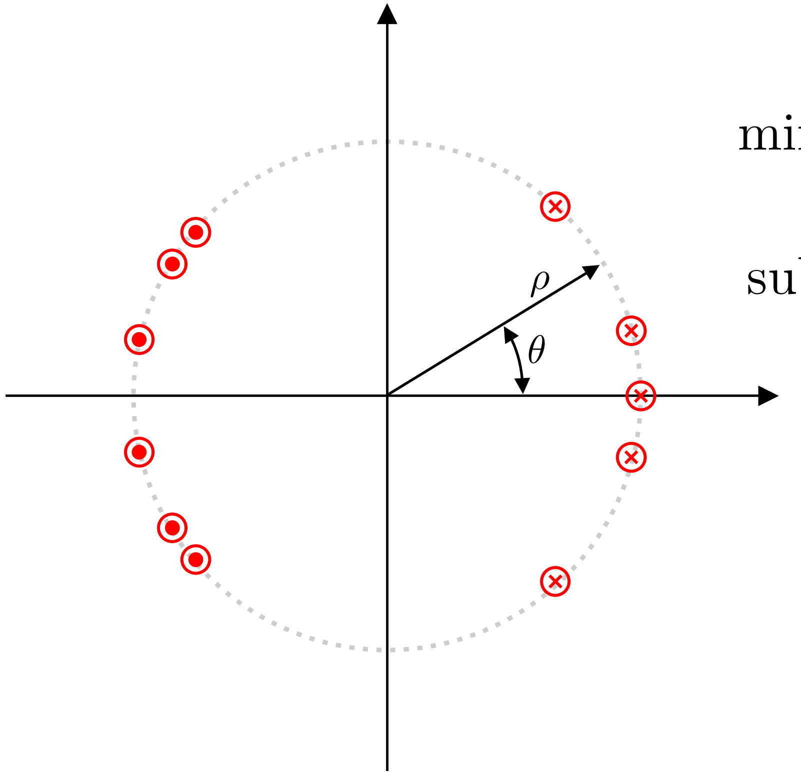

$$\theta = \{\theta_1, \theta_2, \ldots \theta_m\}$$

$$\rho = \{\rho_1, \rho_2, \ldots \rho_m\}$$

$$I = \{I_1, I_2, \ldots I_m\}$$

$$\begin{aligned}
\underset{\theta}{\text{minimize}} \quad & -\sum_{j=1}^{m_{opt}} \cos\theta_j + \sum_{j=m_{opt}+1}^{m_r} \cos\theta_j \\
\text{subject to} \quad & \min\{\|\theta_j - \theta_{j+1}\|\} - \theta_{min} \geq 0, \quad j = 1, \ldots, m_r - 1 \\
& \theta_{min} \leq \theta_j \leq \frac{\pi}{2}, \quad j = 1, \ldots, m_{opt} \\
& \frac{\pi}{2} \leq \theta_j \leq \pi, \quad j = m_{opt}+1, \ldots, m_r \\
& -1 + 2\left(-\sum_{j=1}^{m_{opt}} \cos n\theta_j + \sum_{j=m_{opt}+1}^{m_r} \cos n\theta_j\right) = 0, \quad n = 1, \ldots, n_0
\end{aligned}$$

2. Uni-layer magnets

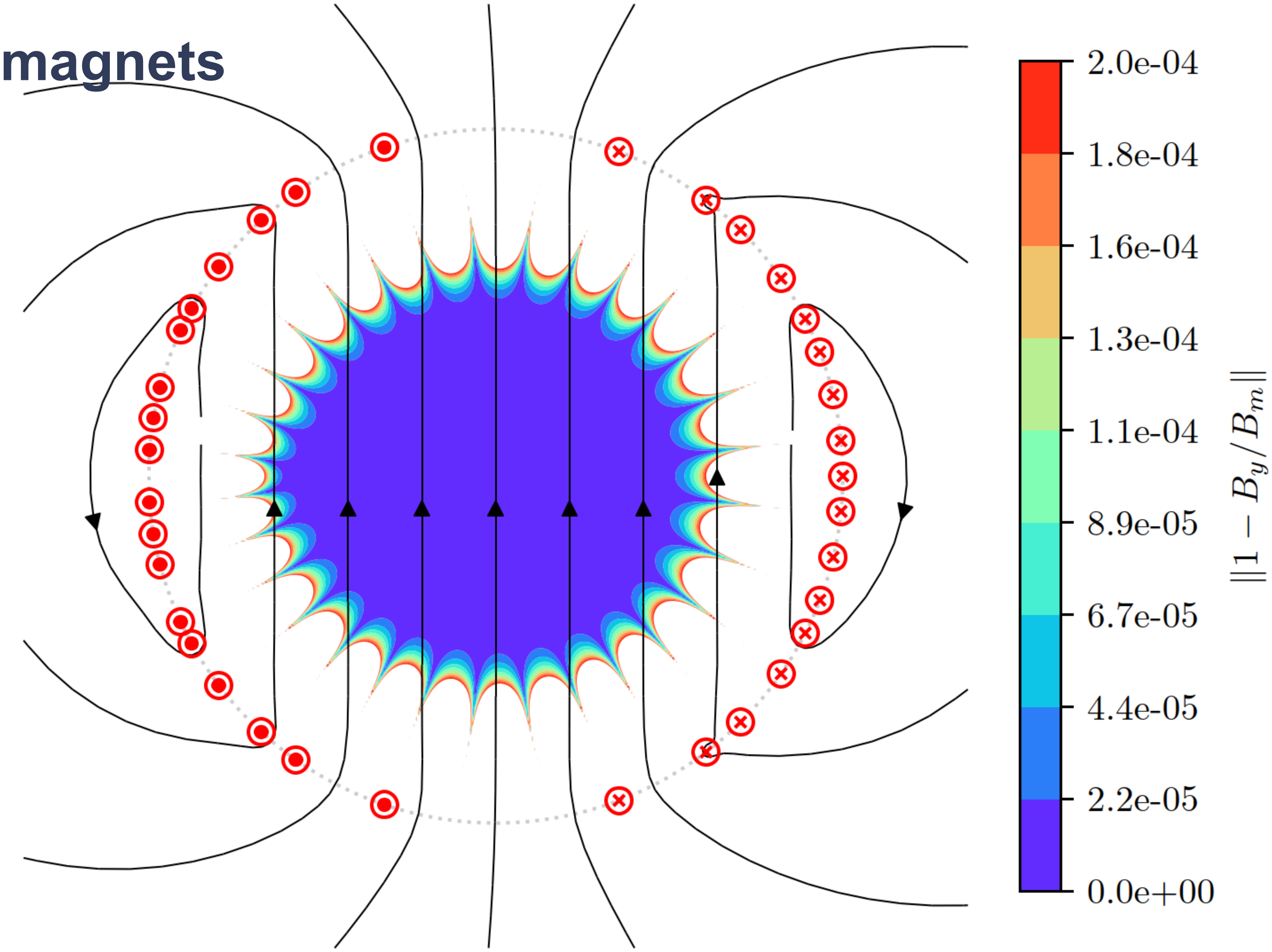

$m_r = 17$, $n_0 = 14$ and $\theta_{min} = 3°$.

2. Uni-layer magnets

Example **asymmetric** solution

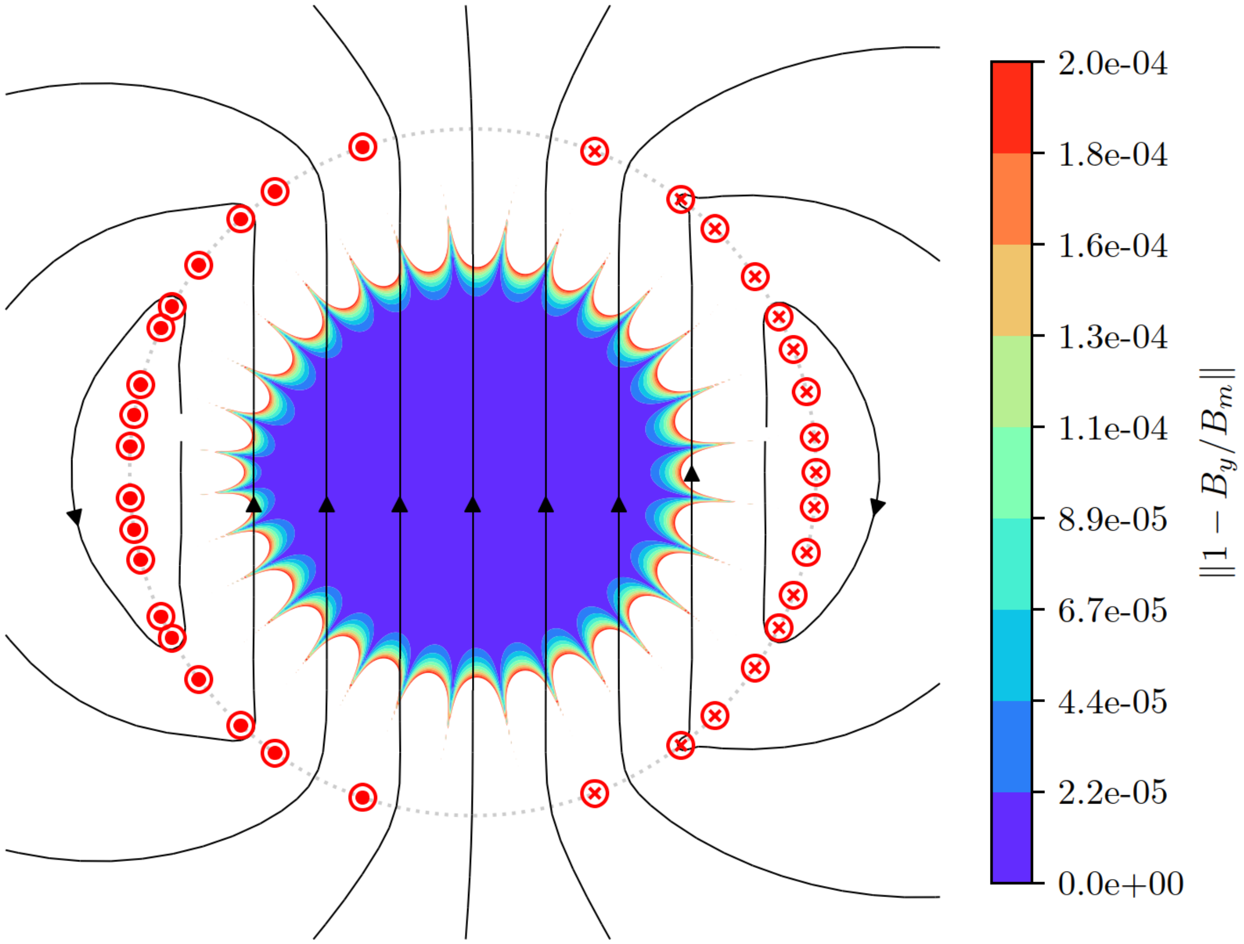

$m_r = 17$, $n_0 = 14$ and $\theta_{min} = 3°$.

Example **symmetric** solution

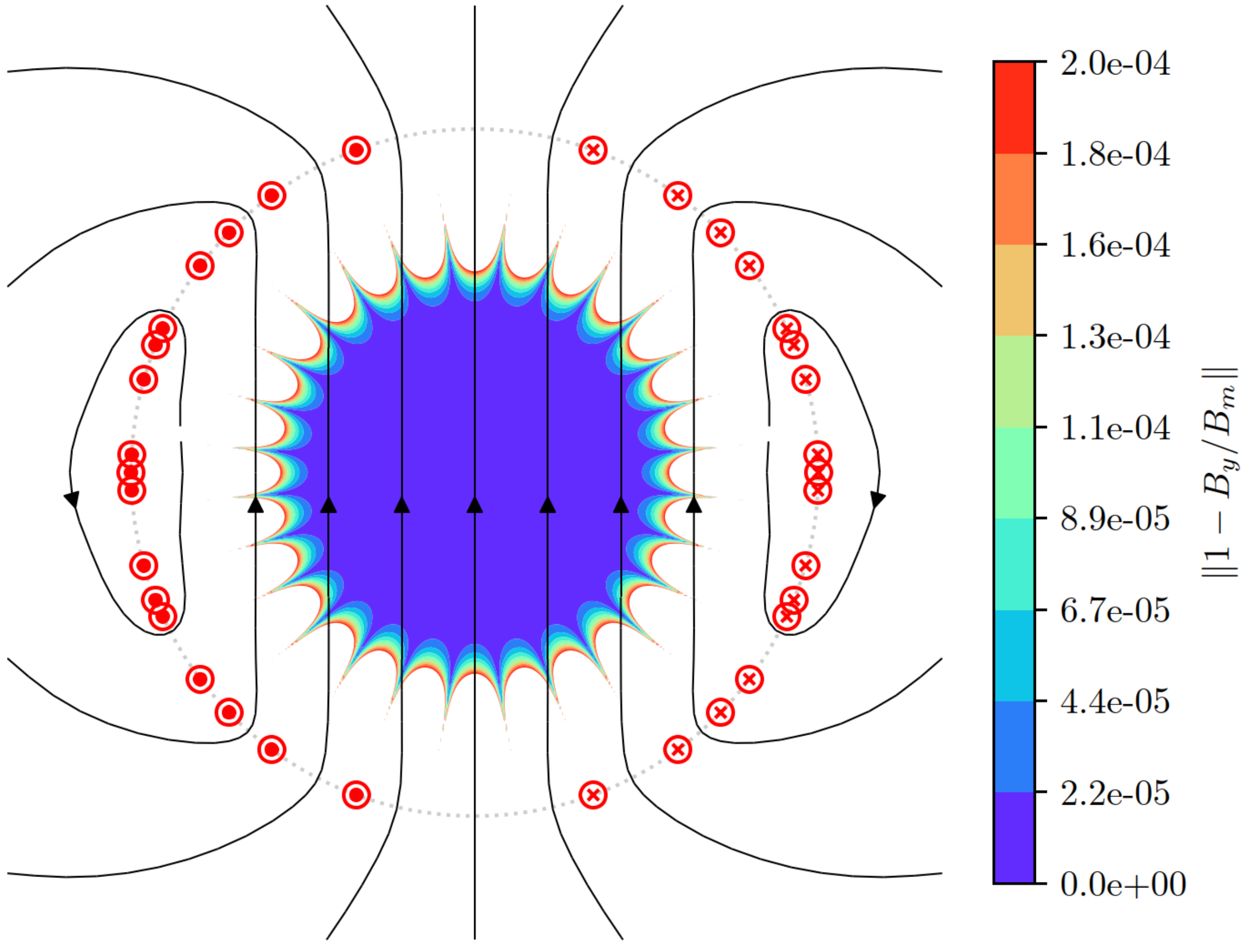

$m_r = 17$, $n_0 = 14$ and $\theta_{min} = 3°$.

2. Uni-layer magnets

Example **asymmetric** solution

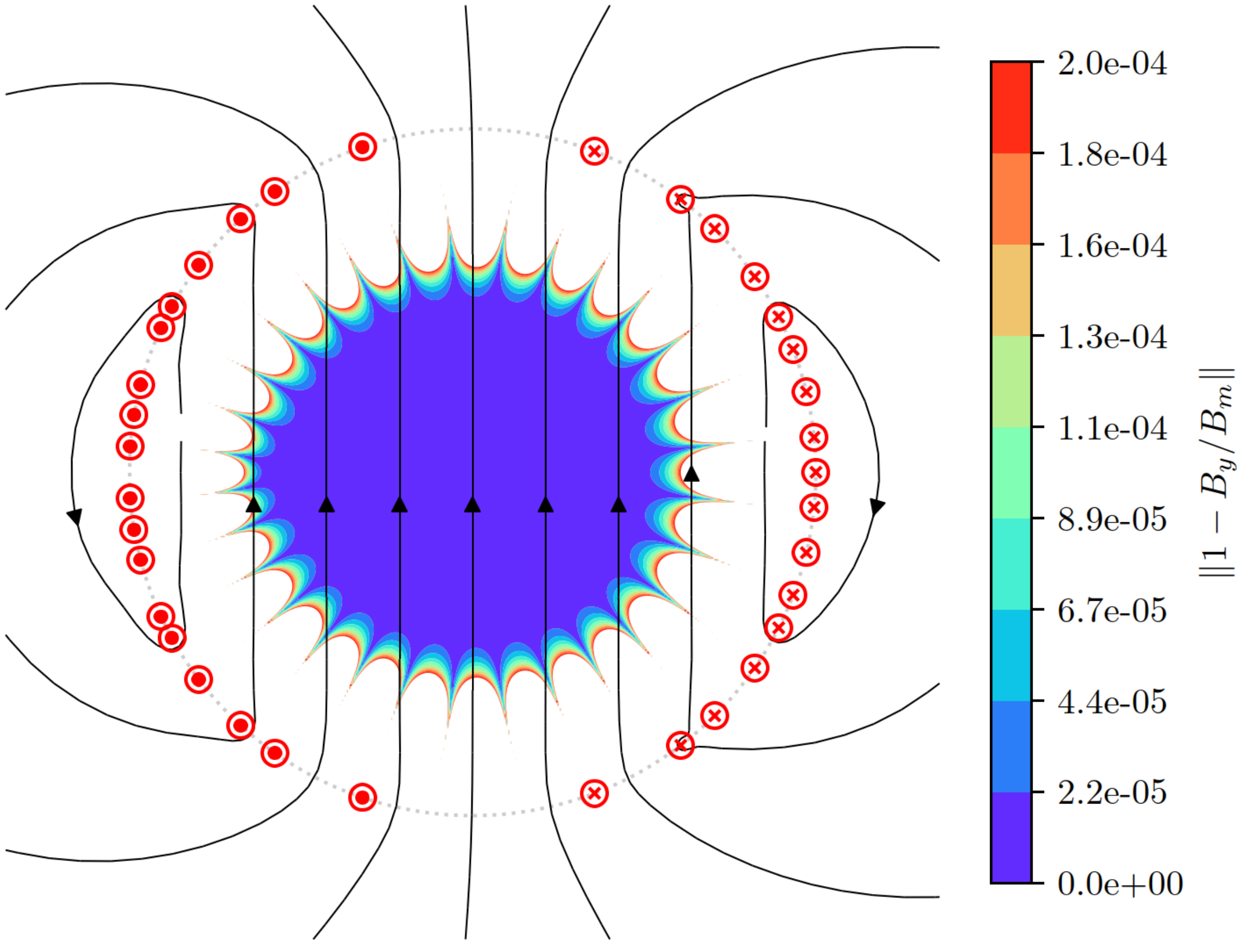

$m_r = 17$, $n_0 = 14$ and $\theta_{min} = 3°$.

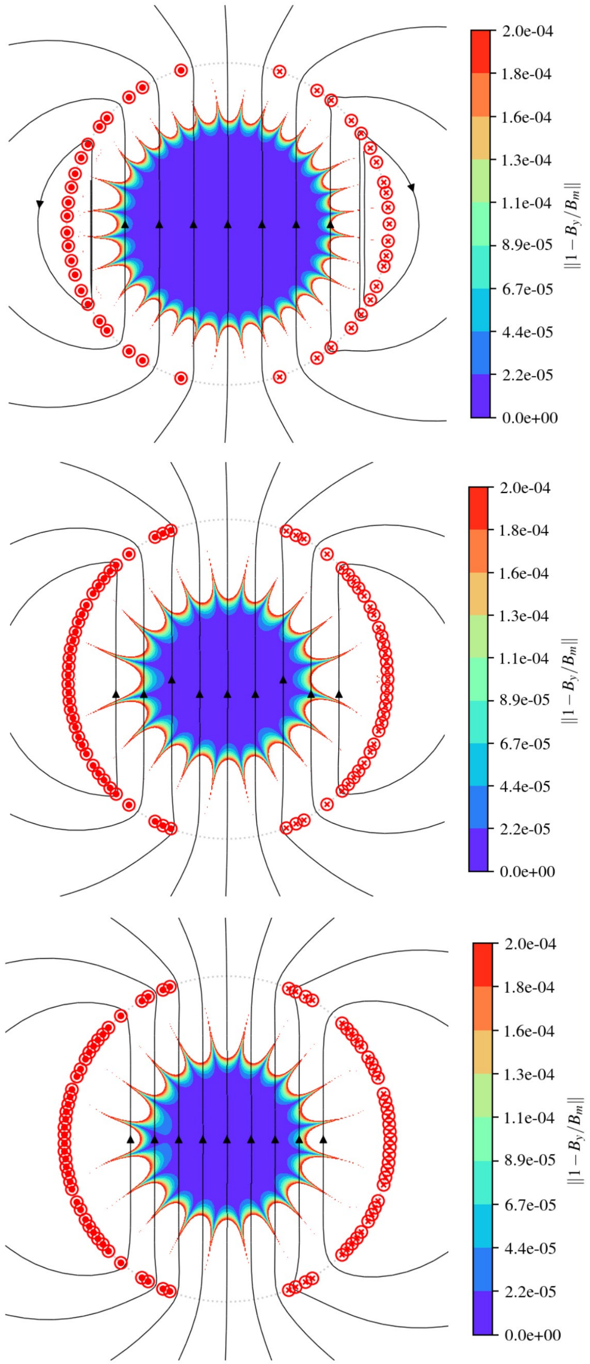

2. Uni-layer magnets

3D Geometry of the magnet

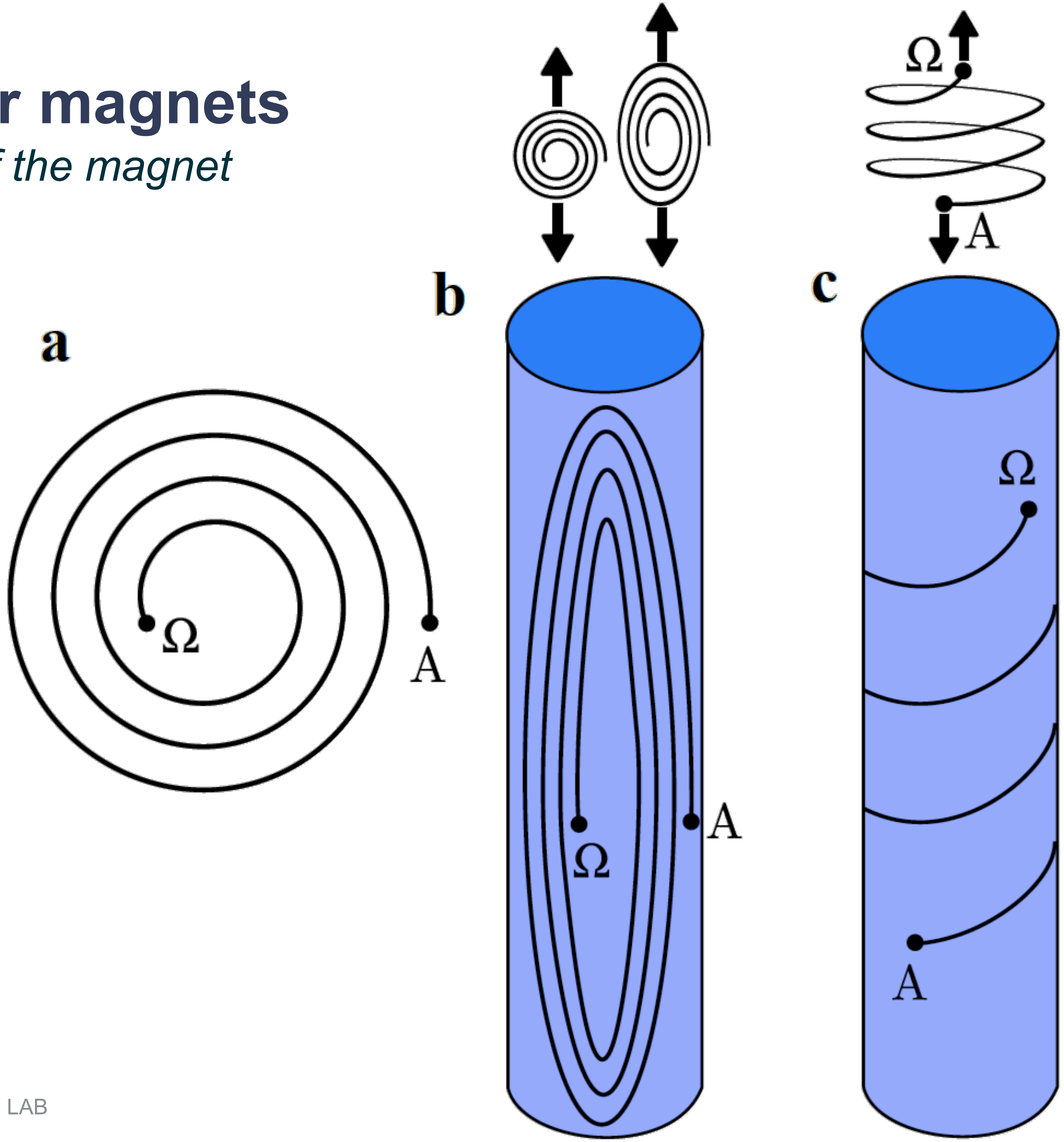

2. Uni-layer magnets

3D Geometry of the magnet

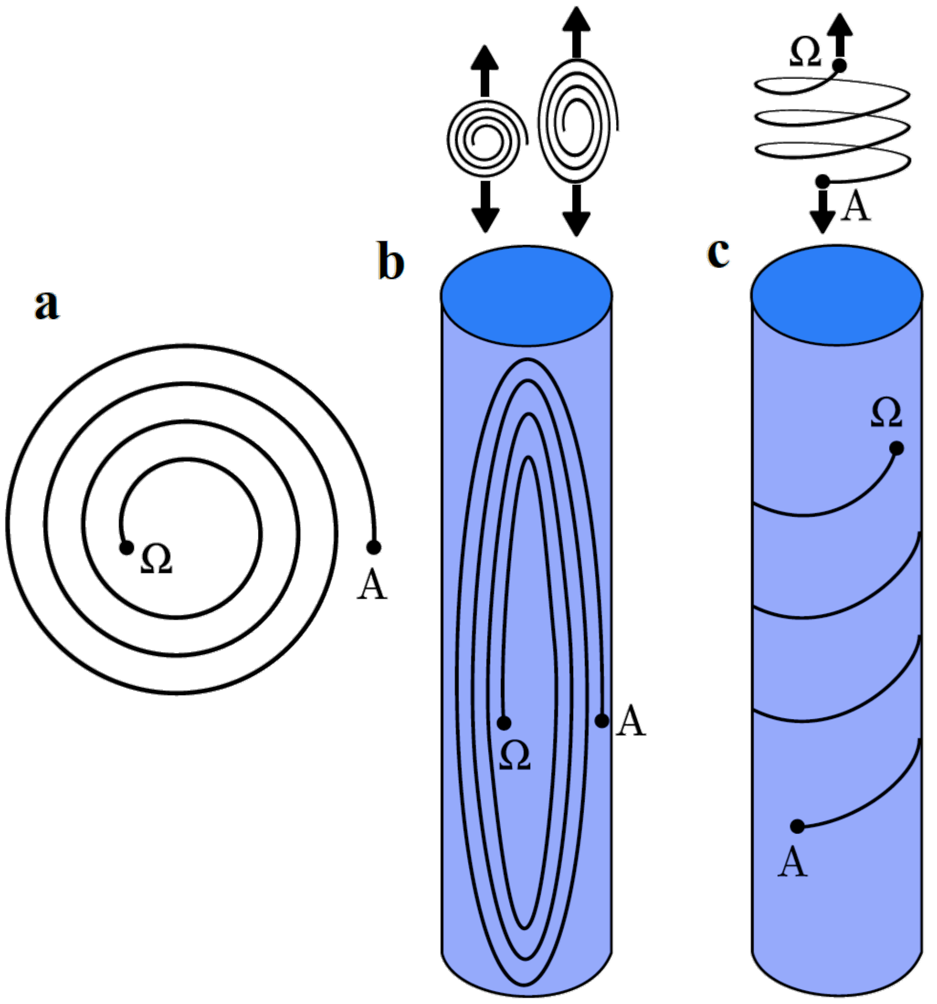

Example **symmetric**

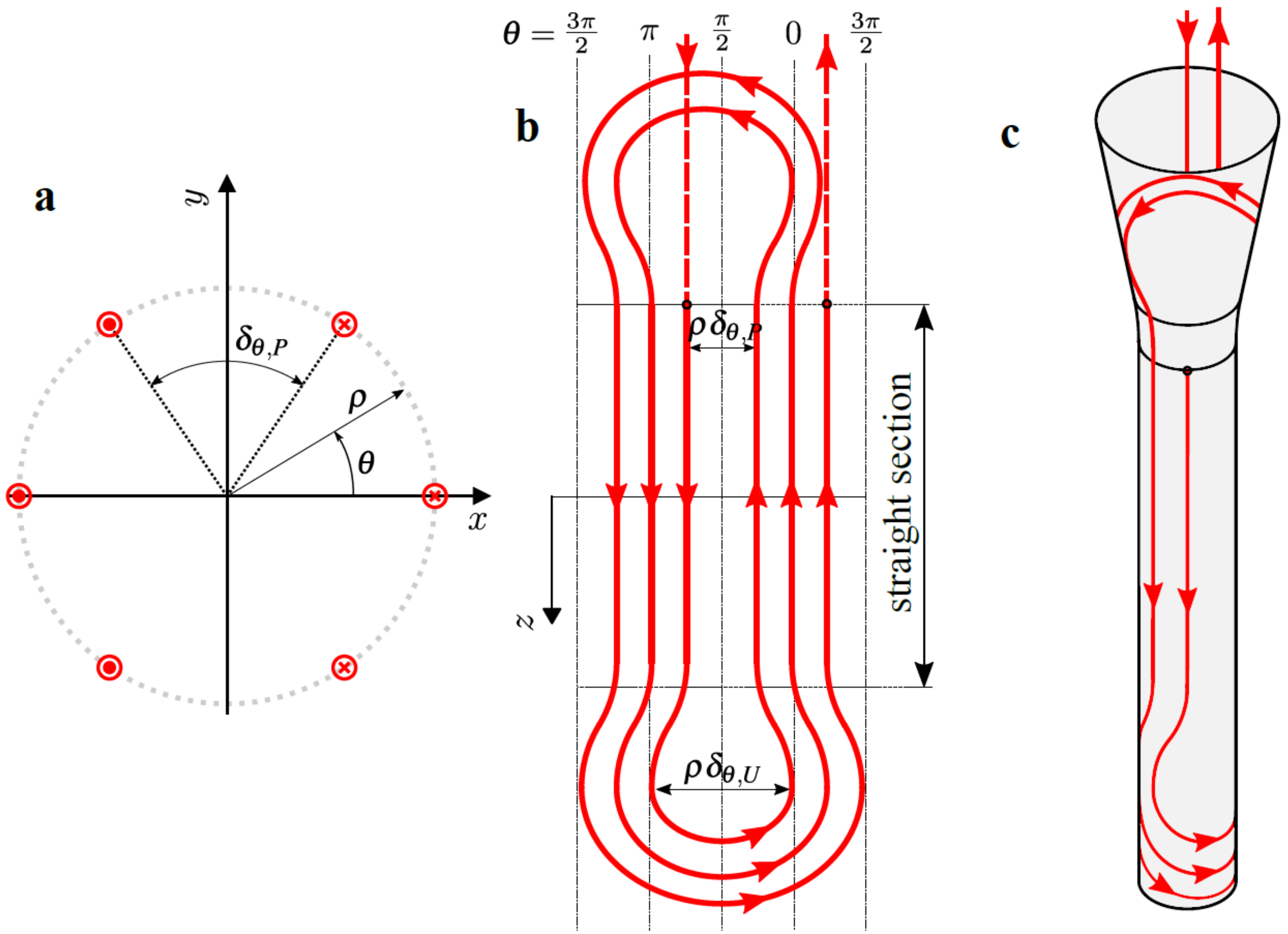

2. Uni-layer magnets – *Surface and winding configuration*

Asymmetric dipole
schematic winding

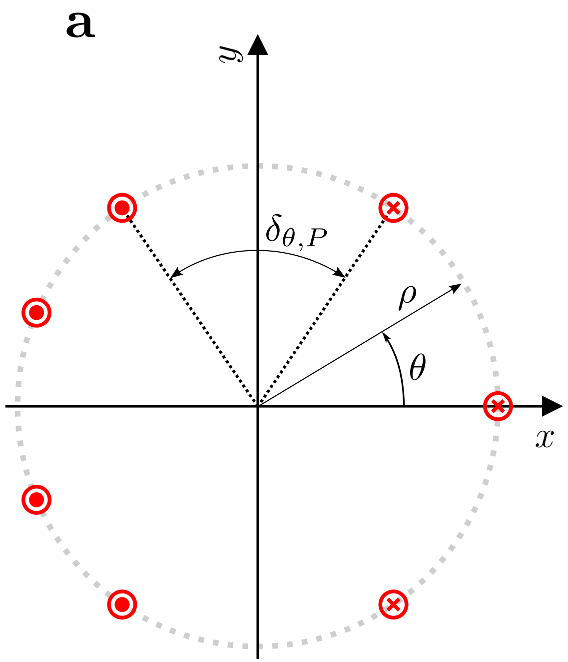

2. Uni-layer magnets – *Surface and winding configuration*

Asymmetric quadrupole
schematic winding

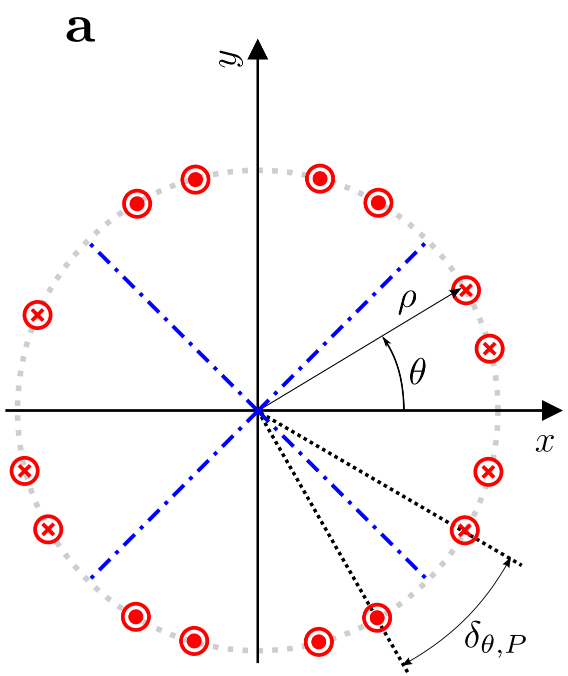

2. Uni-layer magnets – *radius of curvature*

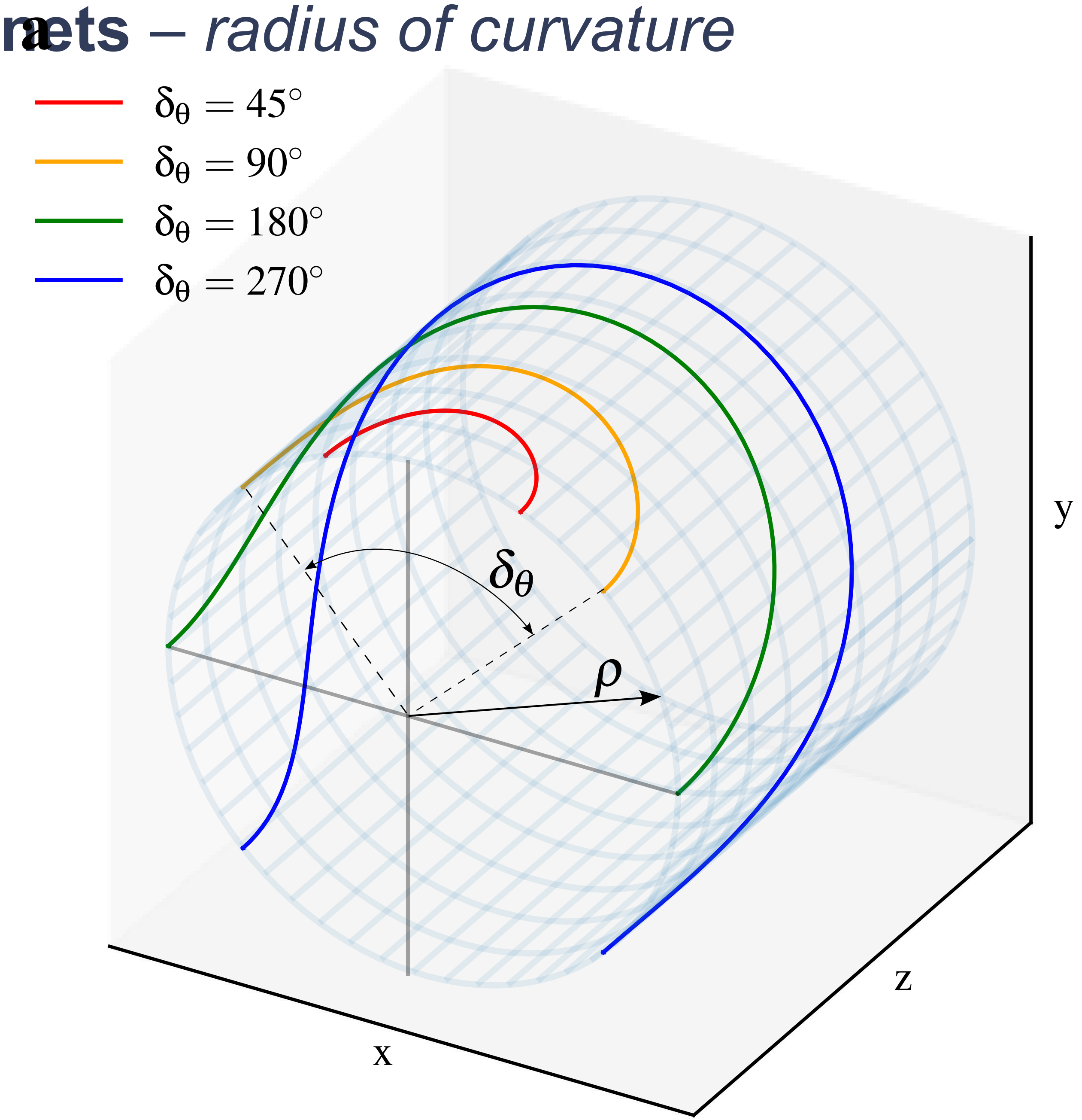

2. Uni-layer magnets – *radius of curvature*

$$\max_{b\in\mathbb{R}|b>0,\zeta\in\mathbb{R}|\zeta\geq 2} \; \min_{\varphi\in(0,\pi/2)} \{R_{min}\}$$

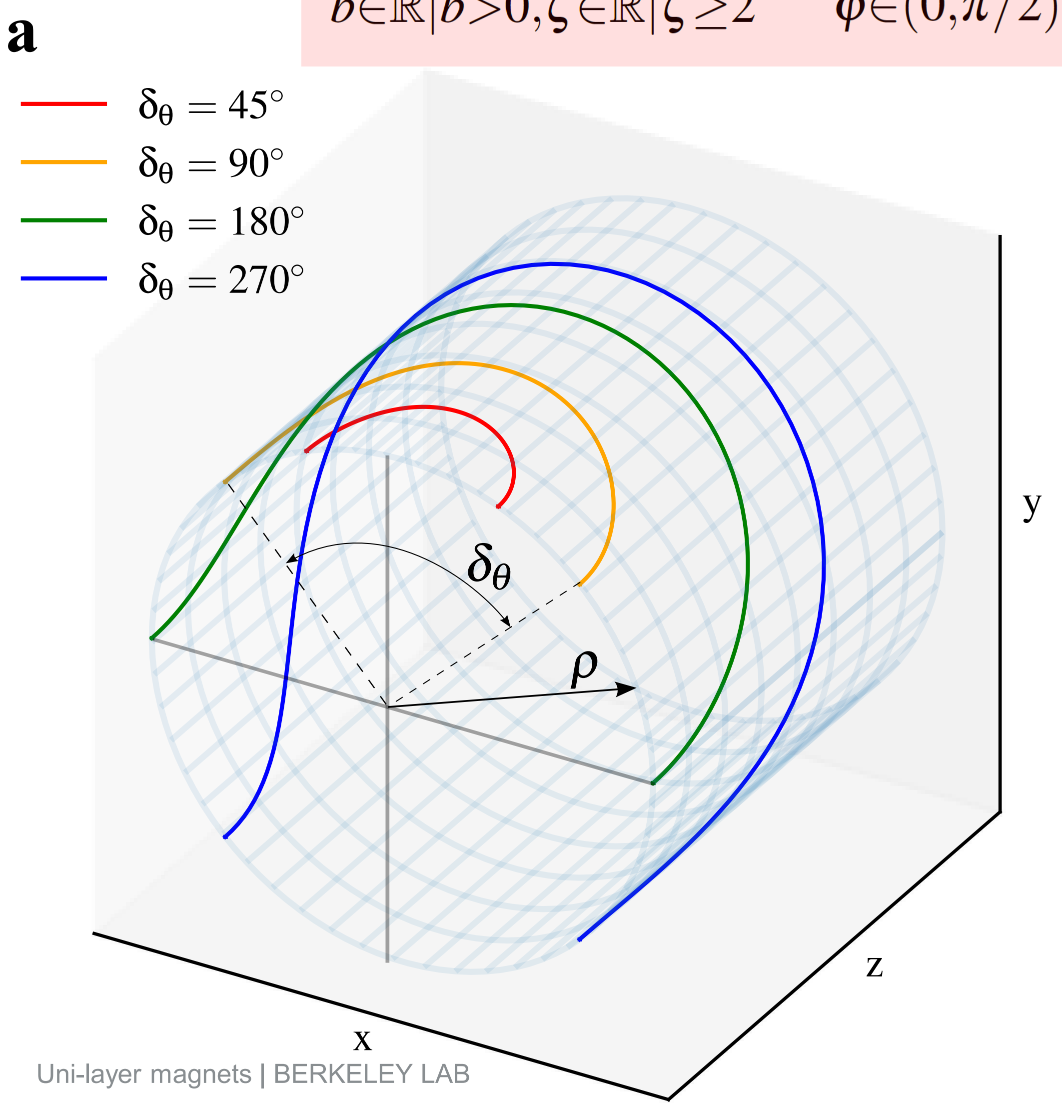

Space curve

$$\gamma_{se}(\varphi) = \rho \sin\left(\frac{a\cos^{\frac{2}{\zeta}}(\varphi)}{\rho}\right)\hat{\mathbf{i}} + \rho\cos\left(\frac{a\cos^{\frac{2}{\zeta}}(\varphi)}{\rho}\right)\hat{\mathbf{j}} + b\sin^{\frac{2}{\zeta}}(\varphi)\hat{\mathbf{k}} \quad \text{with} \quad \varphi \in (0,\pi/2)$$

where

$$a = \rho\frac{\delta_\theta}{2}$$

Radius of curvature

$$R_{se} = \frac{1}{\kappa_{se}} = \frac{\|\gamma_{se}'\|^3}{\|\gamma_{se}' \times \gamma_{se}''\|}$$

$$= \frac{\left(\frac{4b^2\sin^{\frac{4}{\zeta}}(\varphi)}{\tan^2(\varphi)} + \delta_\theta^2\rho^2\cos^{\frac{4}{\zeta}}(\varphi)\tan^2(\varphi)\right)^{\frac{3}{2}}}{\delta_\theta\rho\cos^{-2}(\varphi)} \cdot \left[4b^2\left(\delta_\theta^2\sin^4(\varphi)\cos^{\frac{4}{\zeta}}(\varphi) + 4\zeta^2 - 8\zeta + 4\right)\sin^{-2+\frac{4}{\zeta}}(\varphi)\cos^{2+\frac{4}{\zeta}}(\varphi) + \delta_\theta^4\rho^2\sin^6(\varphi)\cos^{-2+\frac{12}{\zeta}}(\varphi)\right]^{-\frac{1}{2}}$$

2. Uni-layer magnets – *radius of curvature*

$$\max_{b\in\mathbb{R}|b>0,\zeta\in\mathbb{R}|\zeta\geq 2} \quad \min_{\varphi\in(0,\pi/2)} \{R_{min}\}$$

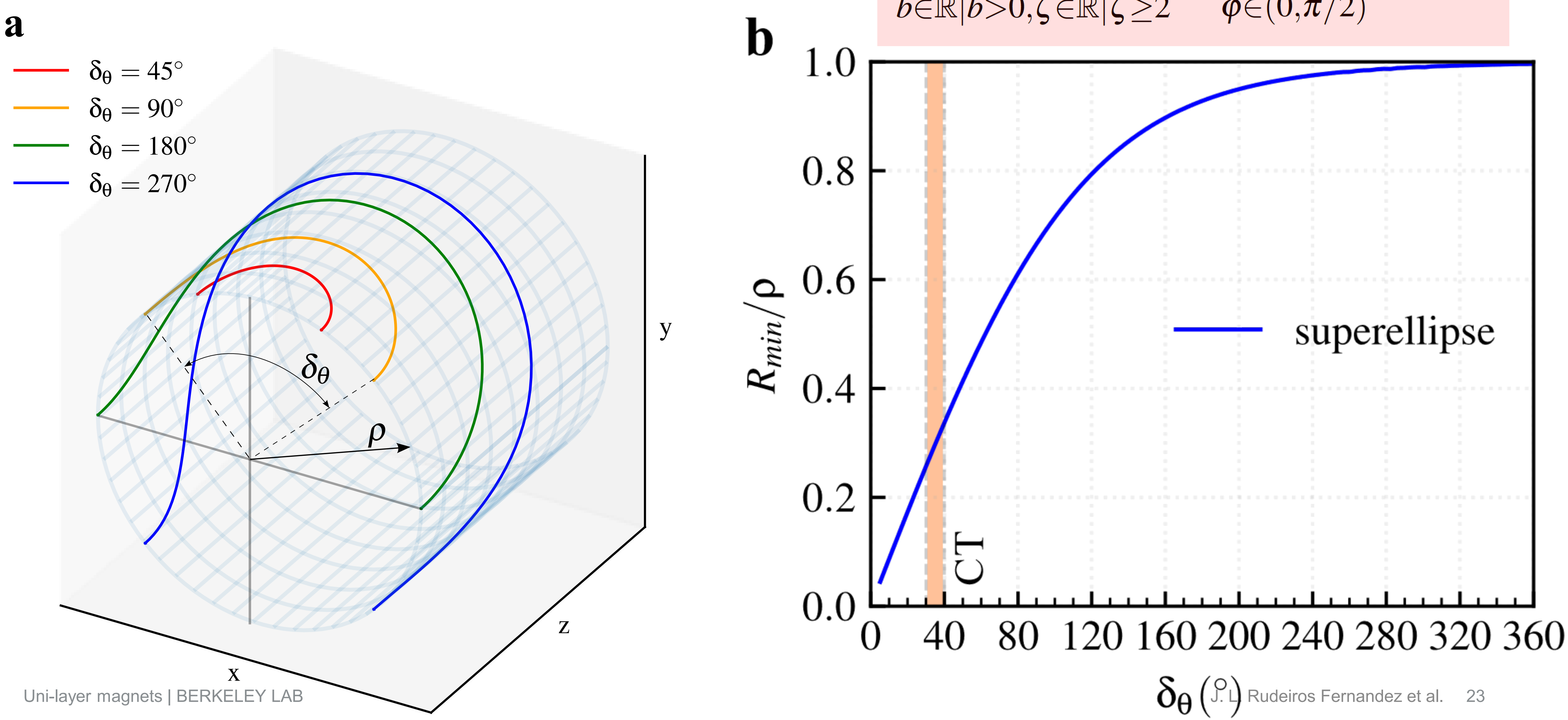

2. Uni-layer magnets – *radius of curvature*

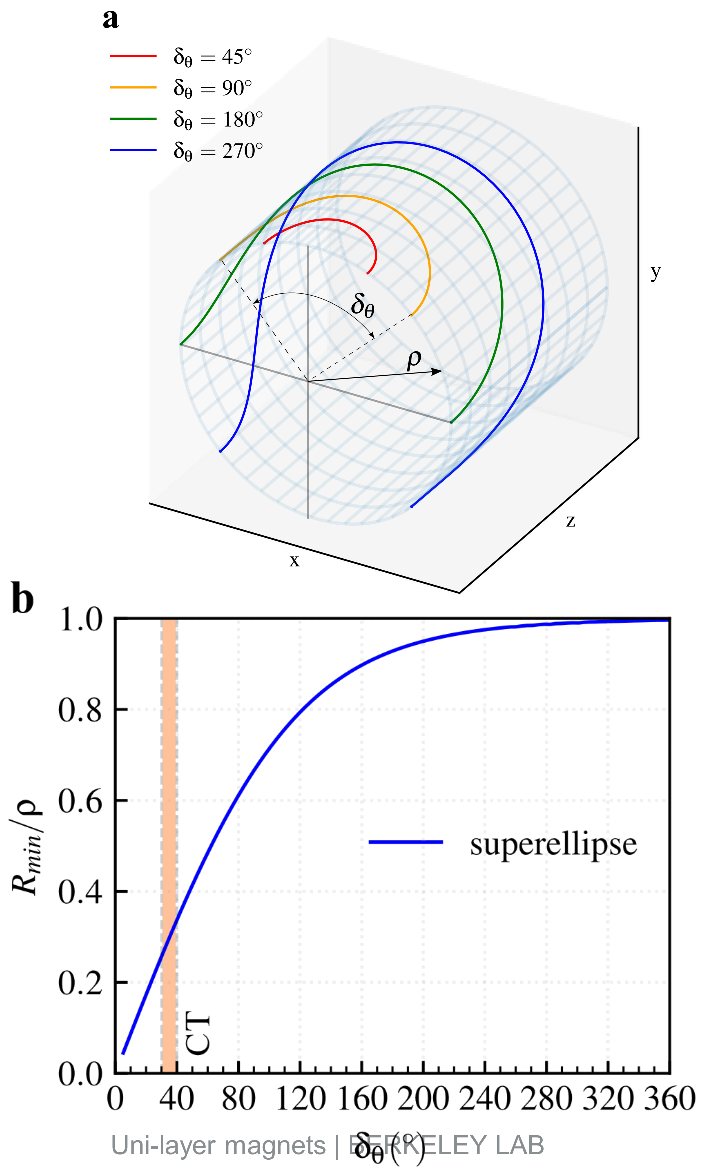

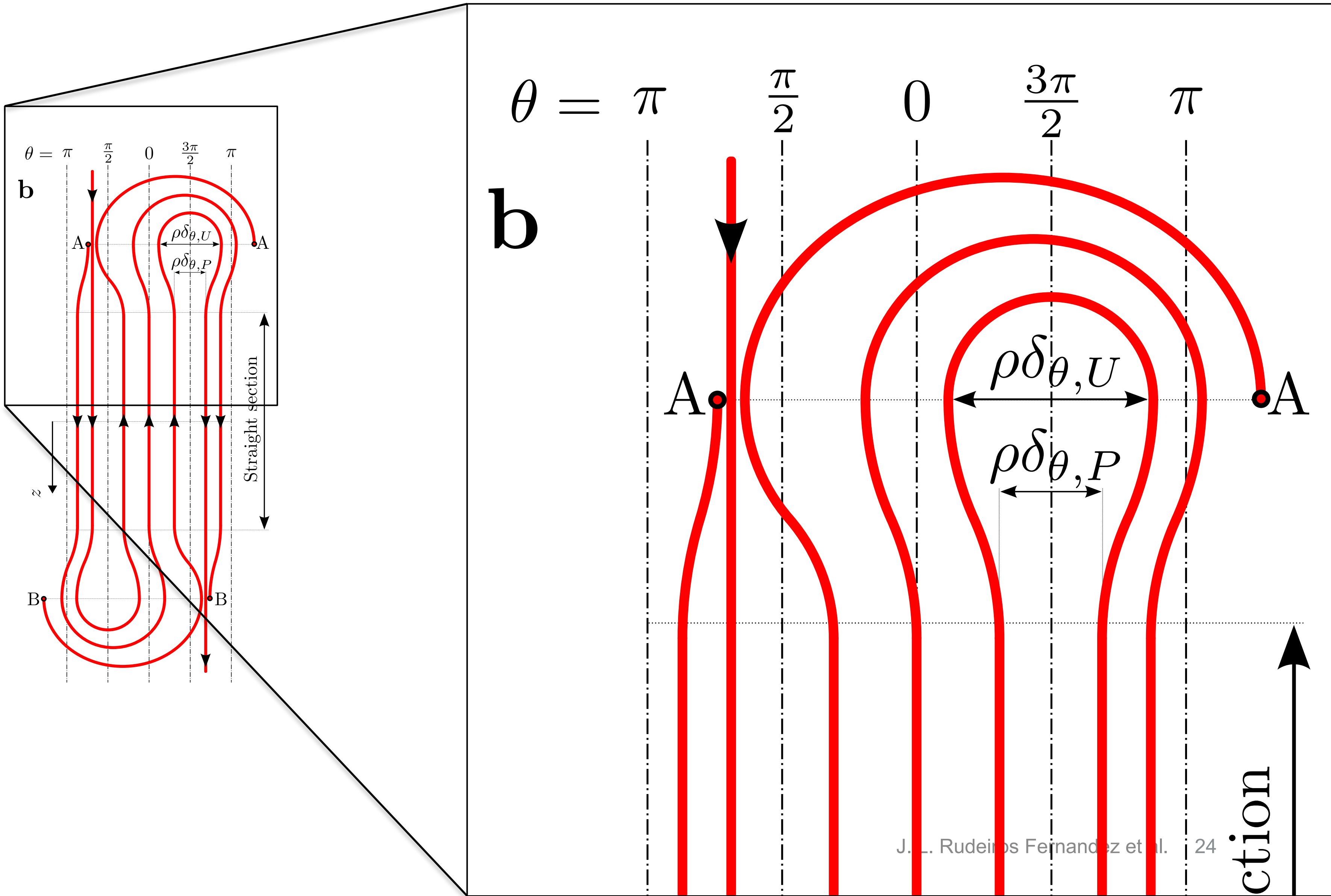

2. Uni-layer magnets – *example solutions*

$$\gamma_{\mathbf{gse}}(\Phi) = \rho\cos\left(\theta_h - \delta_i \sin^{\frac{2}{\chi}}(\Phi)\right)\hat{\mathbf{i}} + \rho\sin\left(\theta_h - \delta_i \sin^{\frac{2}{\chi}}(\Phi)\right)\hat{\mathbf{j}} + \left(z_0 - l_t \cos^{\frac{2}{\zeta}}(\Phi)\right)\hat{\mathbf{k}} \quad \text{with } \Phi \in (0, \pi/2)$$

$$\gamma_{\mathbf{se}}(\varphi) = \rho\sin\left(\frac{a\cos^{\frac{2}{\zeta}}(\varphi)}{\rho}\right)\hat{\mathbf{i}} + \rho\cos\left(\frac{a\cos^{\frac{2}{\zeta}}(\varphi)}{\rho}\right)\hat{\mathbf{j}} + b\sin^{\frac{2}{\zeta}}(\varphi)\hat{\mathbf{k}} \quad \text{with} \quad \varphi \in (0, \pi/2)$$

where

$$a = \rho\frac{\delta_\theta}{2}$$

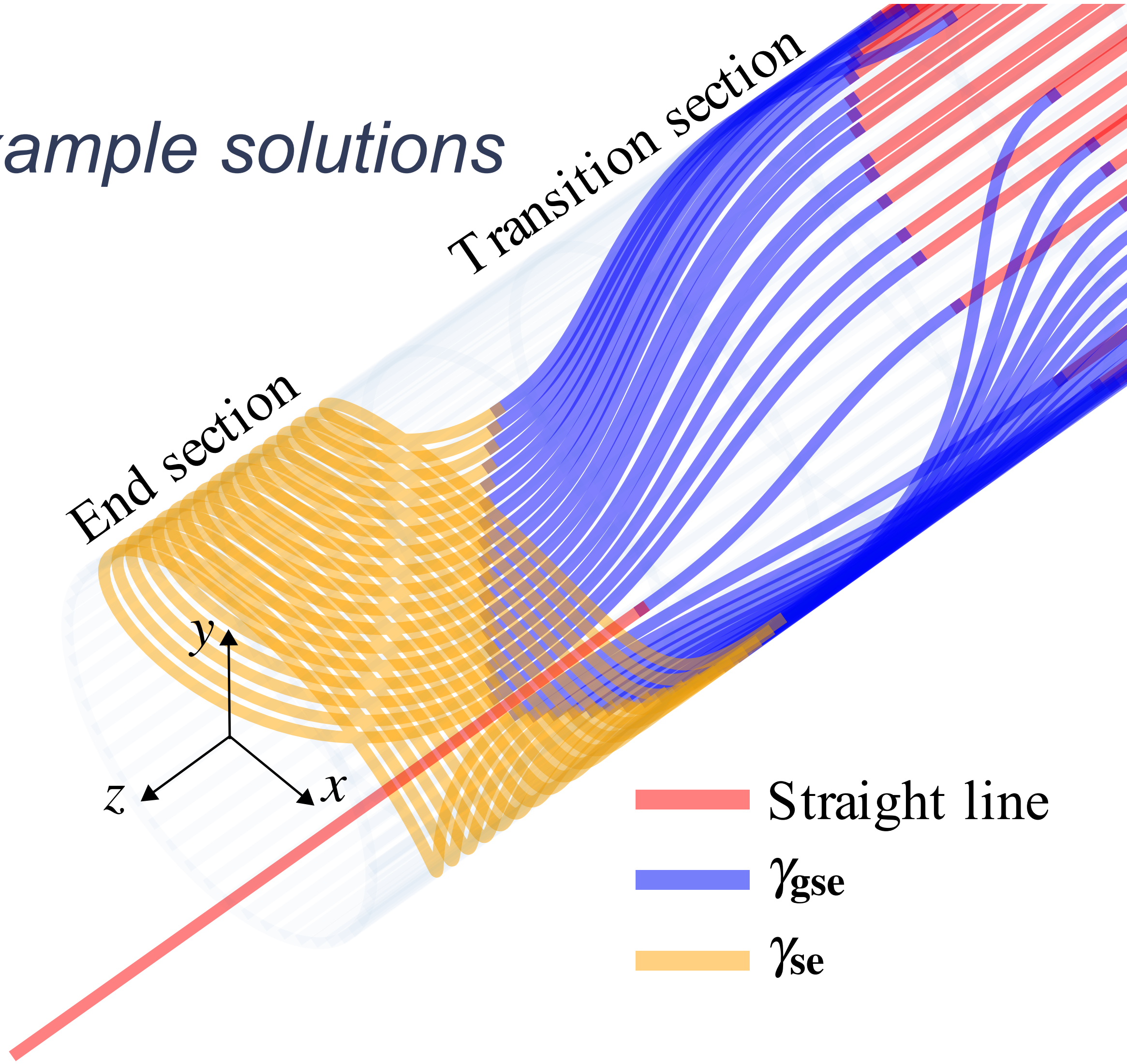

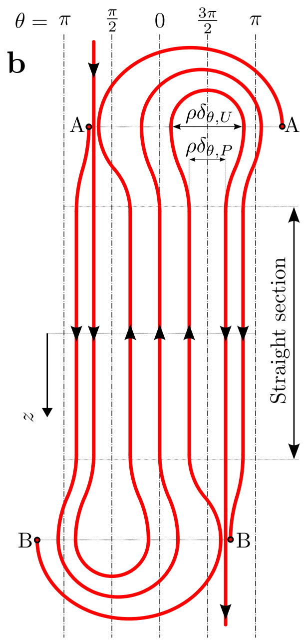

2. Uni-layer magnets – *example solutions*

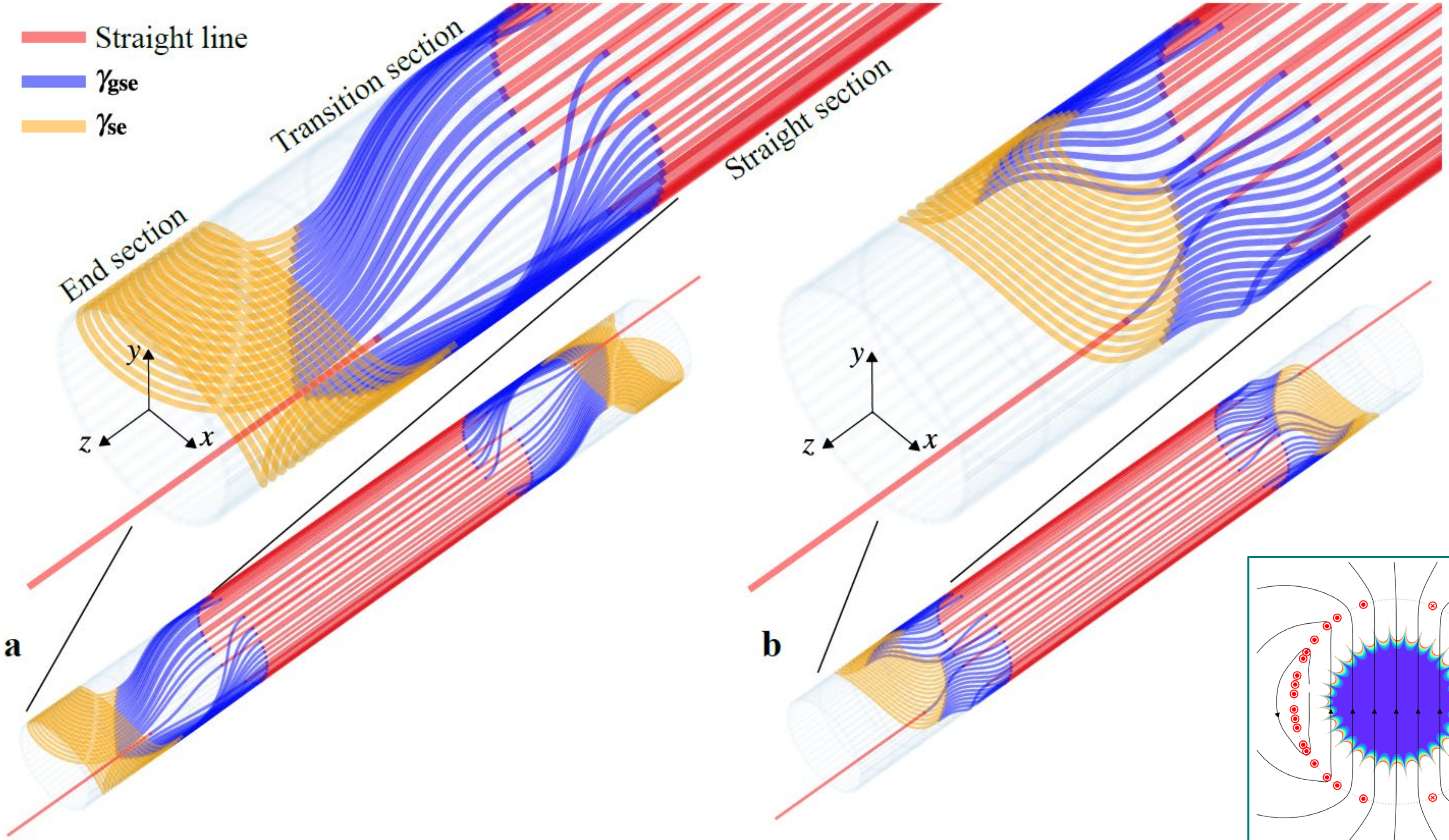

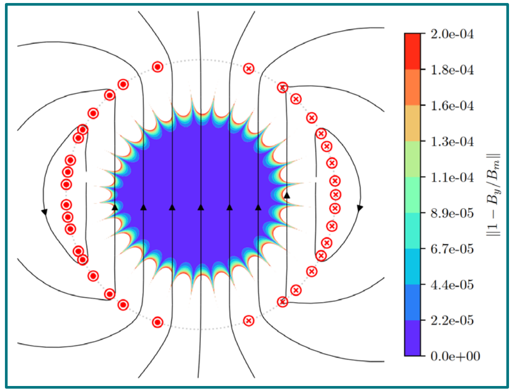

2. Uni-layer magnets – *multi-Uni-layer*

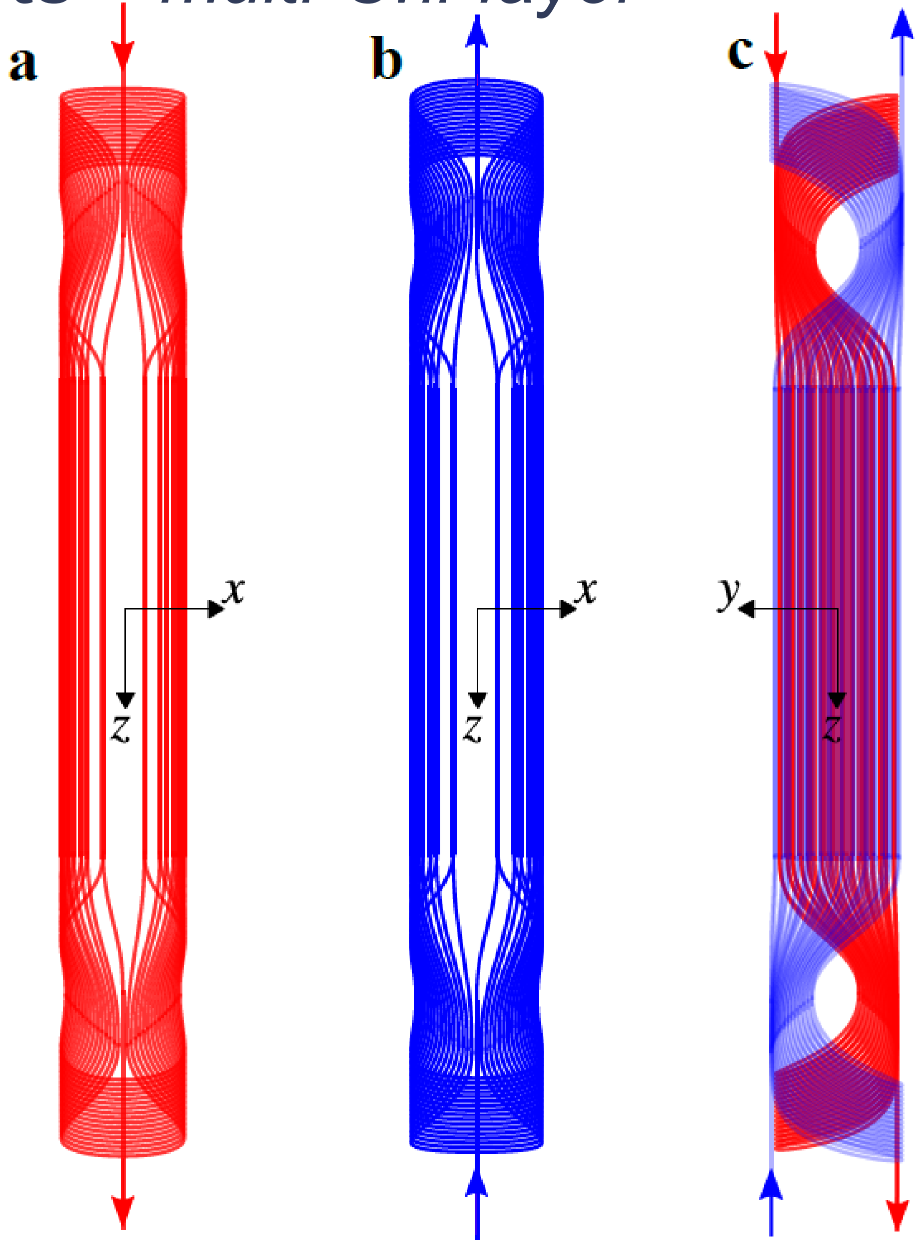

Table of contents

3. Discussion

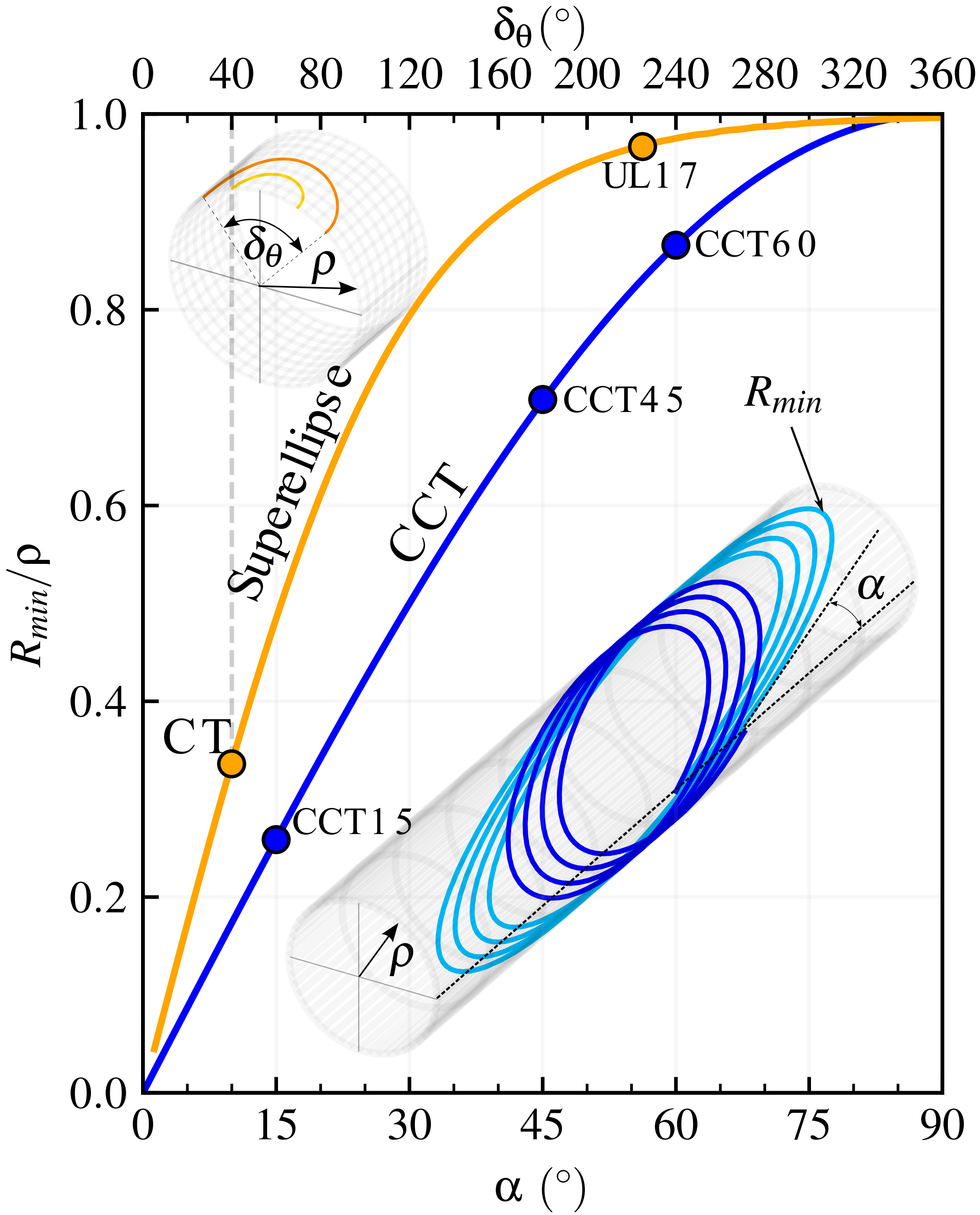

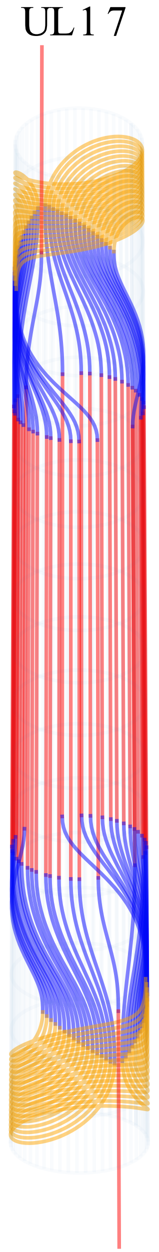

3. Discussion

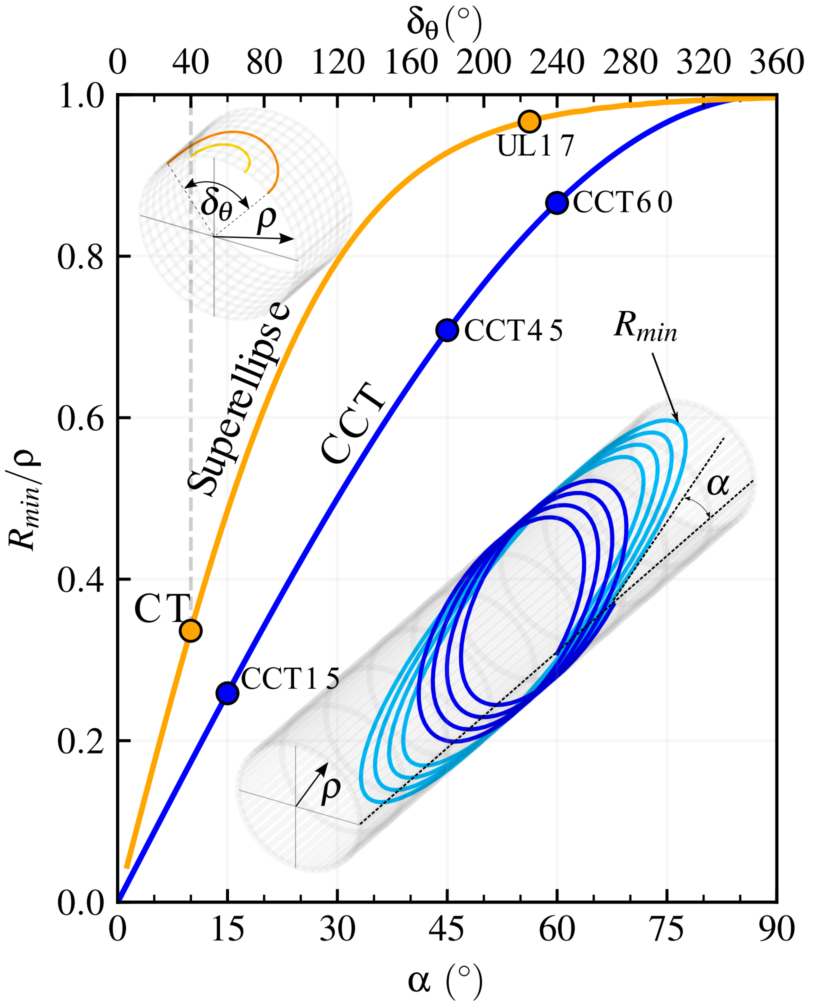

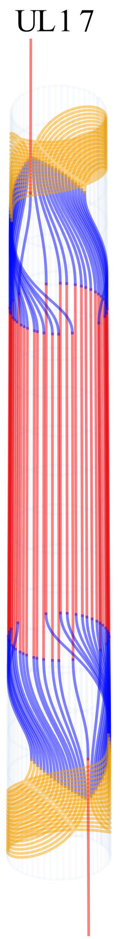

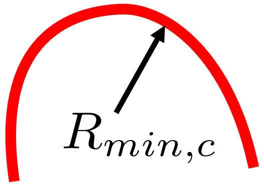

- Same conductor.
- Same length of the conductor.
- Same current.

Smallest possible aperture diameter (i.e. 2*ρ*) that can be wound without degrading the conductor assuming a minimum bending radius of $R_{min,c}$ = 25 mm (i.e. similar to CORC® wire).

Coil design	Smallest possible aperture (mm)	Dipole field transfer function for the same constant length of conductor across all coil designs (T/kA)	Central field ratio ($B_m/B_{m,UL17}$)
UL (UL17)	51	0.218	1
CT (δ_θ = 40°)	147	0.075	0.34
CCT (α = 15°)	192	0.051	0.23
CCT (α = 45°)	71	0.081	0.37
CCT (α = 60°)	58	0.064	0.29

3. Discussion

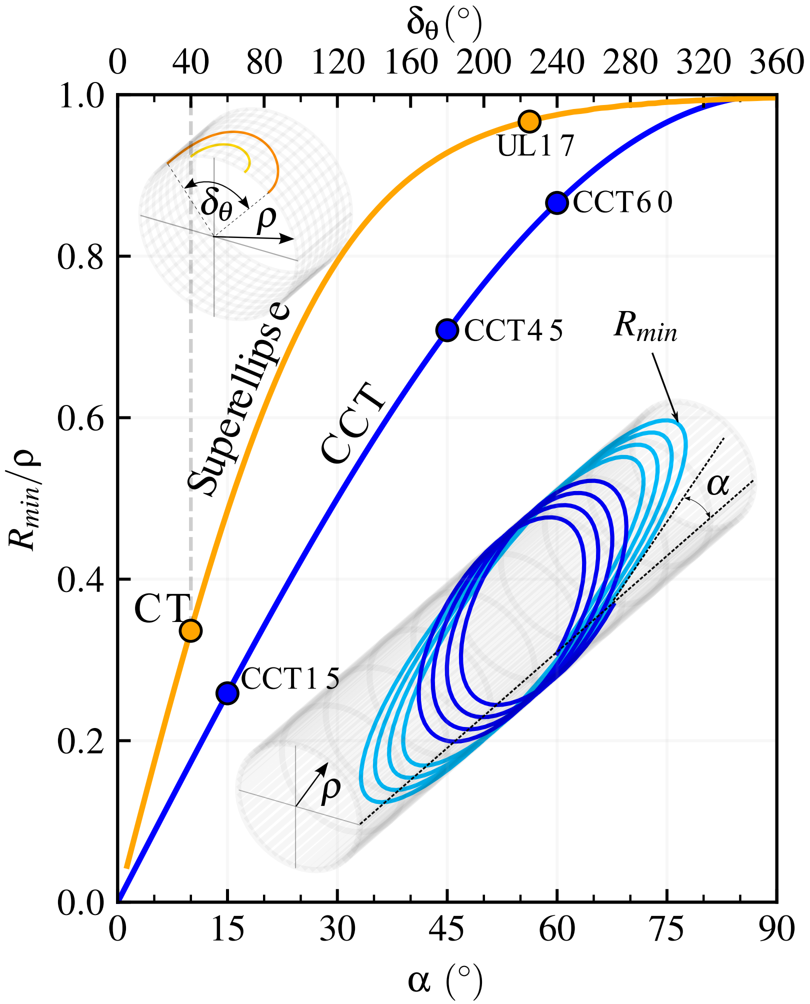

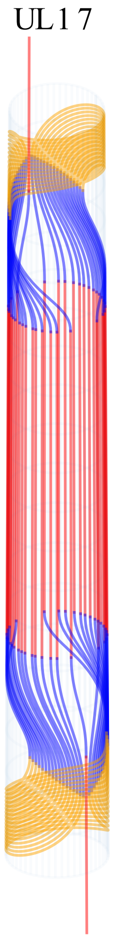

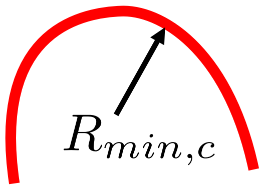

- Same conductor.
- Same length of the conductor.
- Same current.

Minimum radius of curvature R_{min} required in the conductor to wind a coil with an aperture of 50 mm.

Coil design	Minimum radius of curvature (mm)	Dipole field transfer function for the same constant length of conductor across all coil designs (T/kA)	Central field ratio ($B_m/B_{m,UL17}$)
UL (UL17)	24	0.222	1
CT (δ_θ = 40°)	8.5	0.222	1
CCT (α = 15°)	6.5	0.197	0.89
CCT (α = 45°)	17	0.115	0.52
CCT (α = 60°)	21	0.075	0.34

3. Discussion - Fabrication

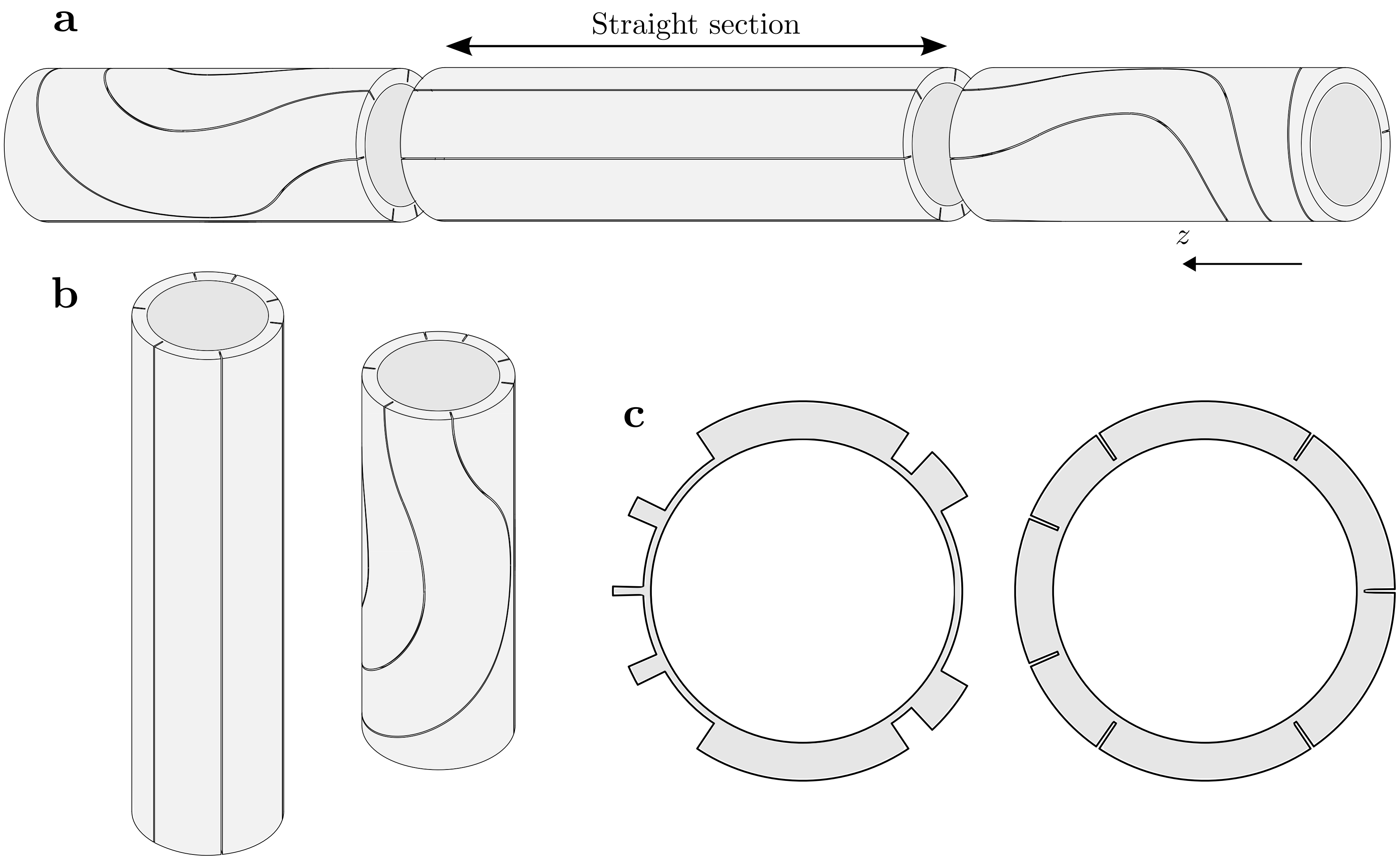

3. Discussion

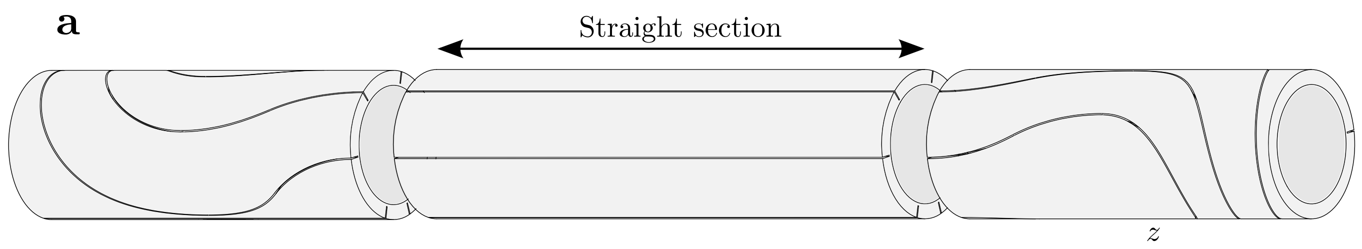

Some thoughts:

- Significant increase in the minimum bending radius required in the conductor, compatible with REBCO-based CORC wire.
- Minimization of overall required tooling for manufacturing (similar to CCT).
- Relative simplification of manufacturing of the mandrel in relation to other stress-managed structures.
- Reduced required effort in metrology and magnet assembly (no half to close the aperture).
- Possibility of field quality measurements and cold testing of individual layers before magnet assembly.
- Elimination of internal layer jumps and enhanced potential for layer-to-layer grading.
- Compact combined function magnets.

4. Conclusions

- The novel concept of **Uni-layer** magnets has been presented.
- The asymmetric Uni-layer magnet presents significant advantages over other concepts, merging the advantages of the costheta and CCT concepts, providing a high-quality field in terms of harmonics, within a **single-layer** (no internal layer jumps), using a single continuous conductor, and with a **higher minimum radius of curvature** required in the conductor during winding.
- This new concept is especially advantageous in the domain of stress-managed magnets for HTS conductors.

Thank you!!!

Rudeiros Fernández et al 2023 Supercond. Sci. Technol.
https://doi.org/10.1088/1361-6668/acc281

$$\mathbf{B}(z) = B_y(x,y) + iB_x(x,y) \quad \text{where} \quad z = x + iy$$

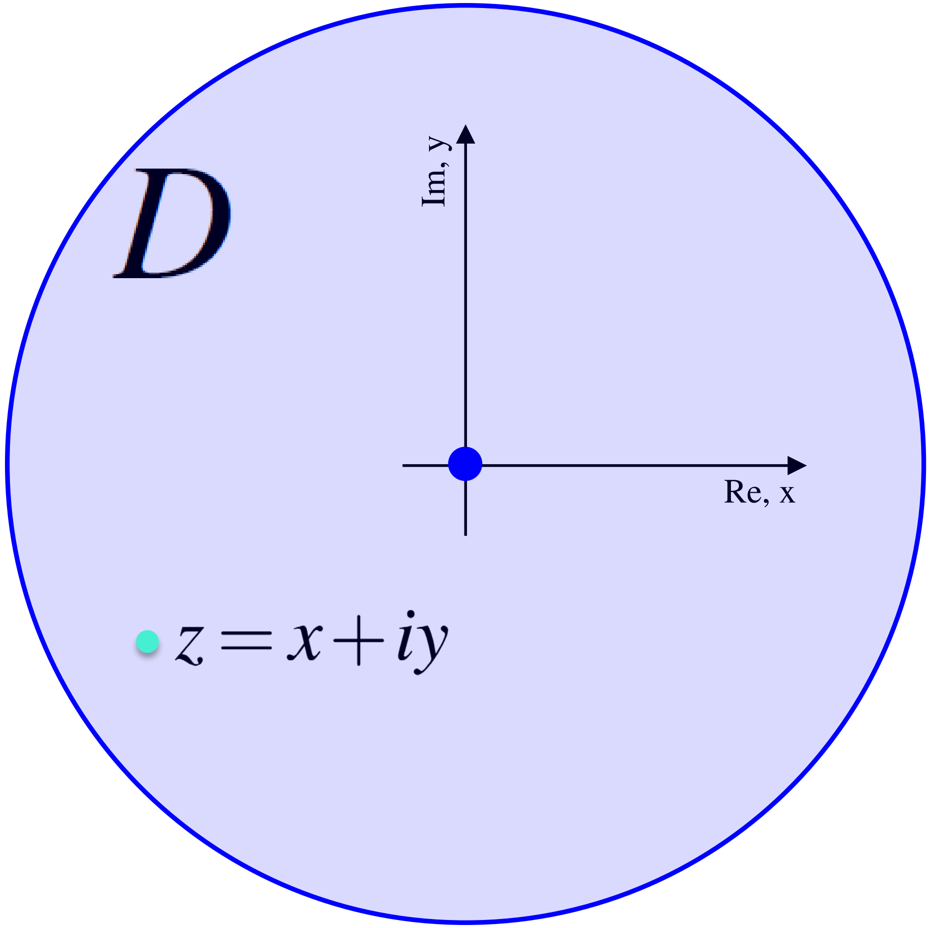

$$\mathbf{B}(z) = \sum_{n=1}^{\infty} C_n \left(\frac{z}{R_{ref}} \right)^{n-1} \quad \text{with} \quad z \in D$$

$$C_n = B_n + iA_n$$

$$\mathbf{B}(z) = \sum_{n=1}^{\infty} C_n \left(\frac{z}{R_{ref}} \right)^{n-1} \quad \text{with} \quad z \in D$$

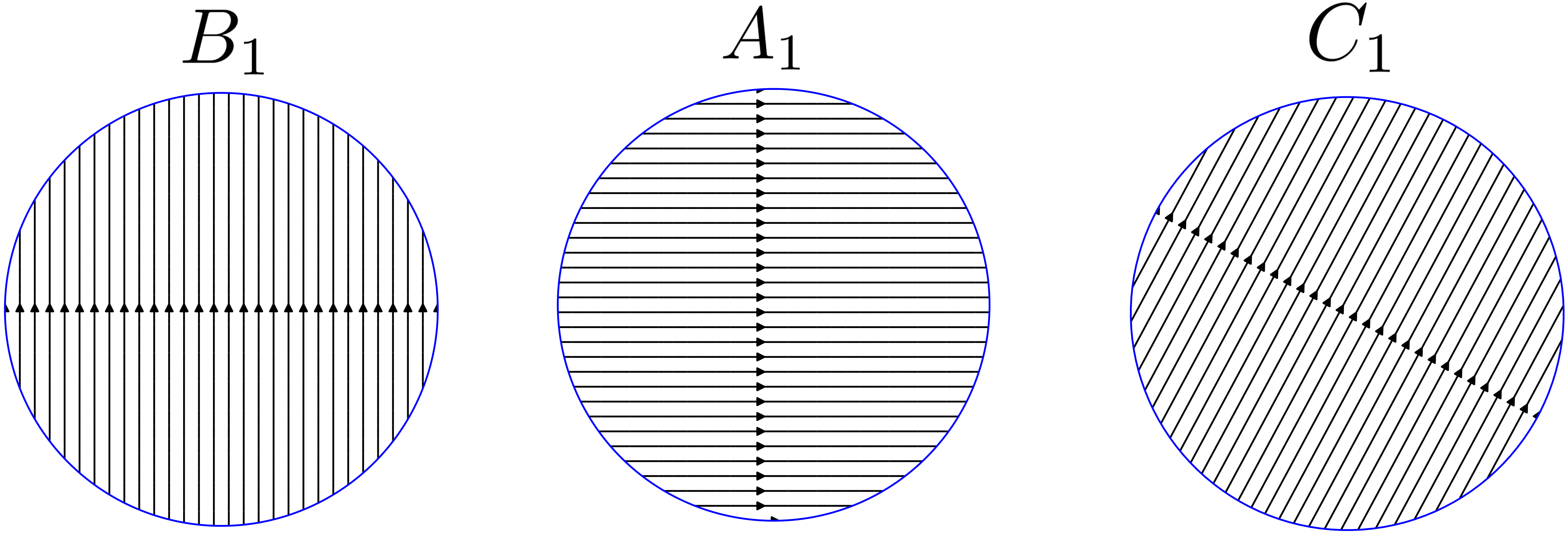

$$z = x + iy$$

$$\mathbf{B}(z) = \frac{\mu_0 I}{2\pi} \frac{1}{z - z_s}$$

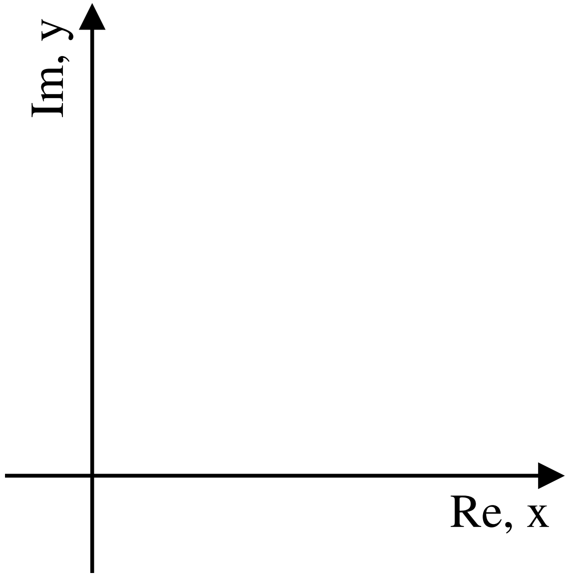

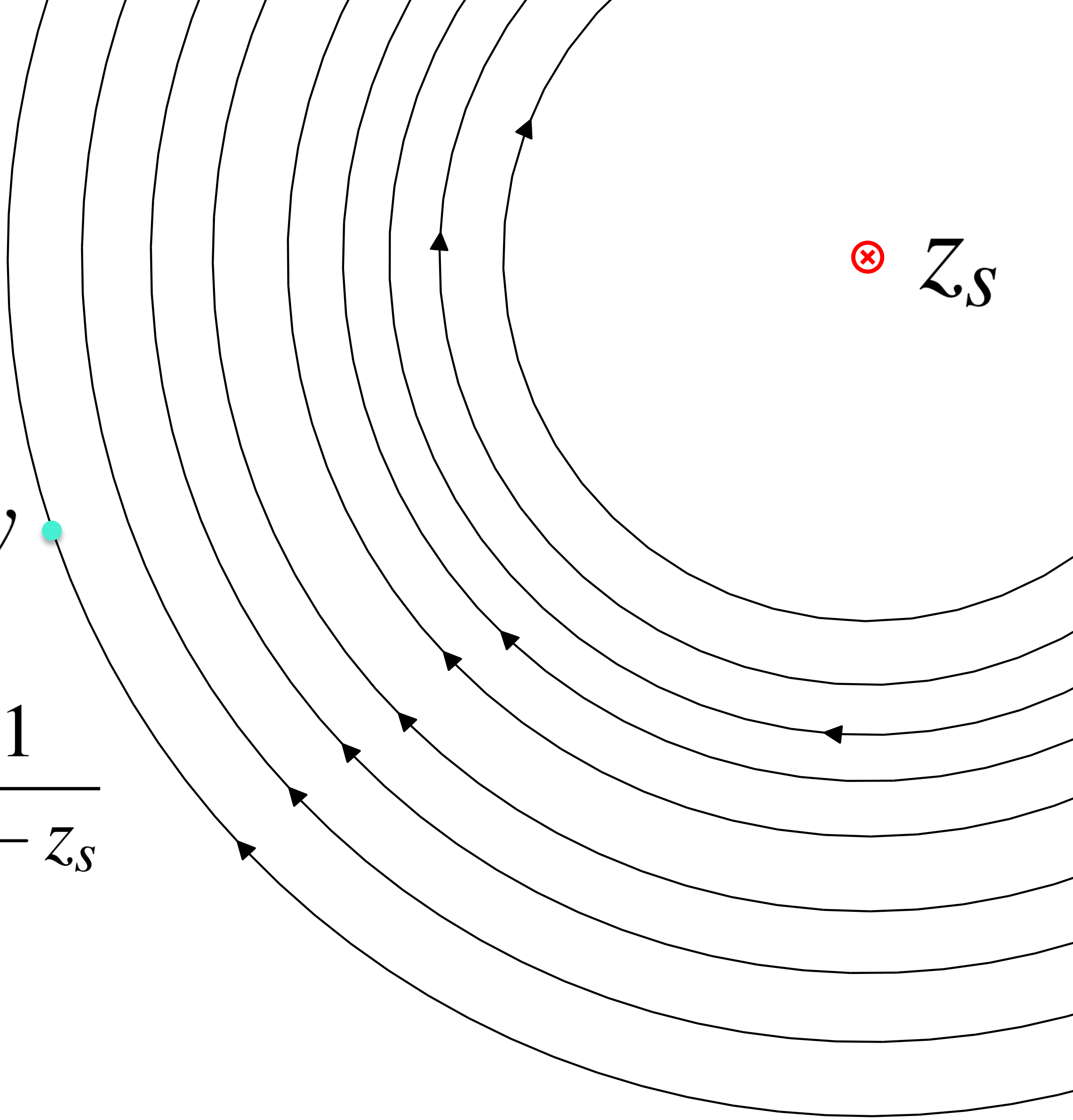

$$\mathbf{B}(z) = \frac{\mu_0 I}{2\pi} \frac{1}{z - z_s}$$

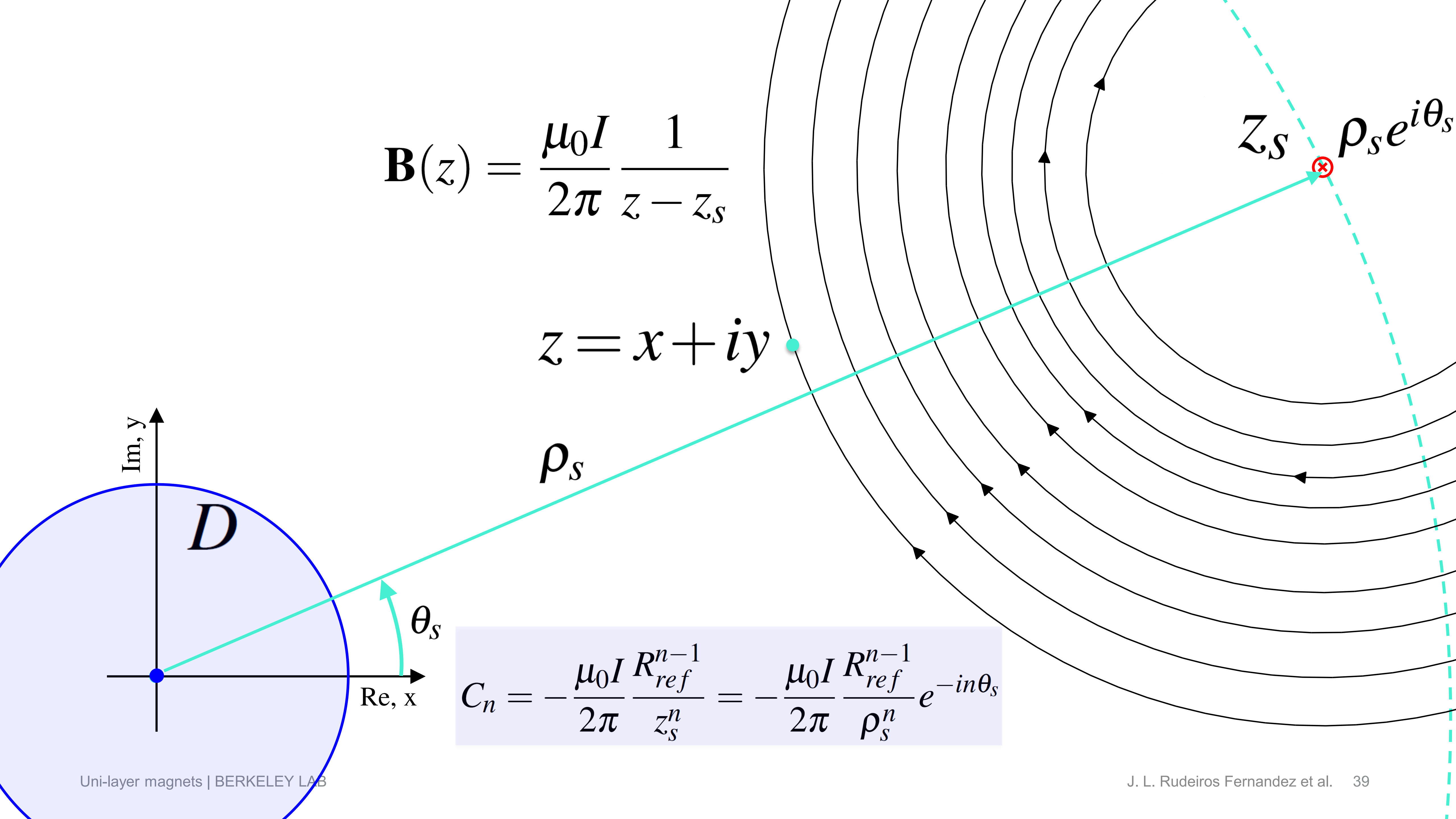

$$C_n = -\frac{\mu_0 I}{2\pi} \frac{R_{ref}^{n-1}}{z_s^n} = -\frac{\mu_0 I}{2\pi} \frac{R_{ref}^{n-1}}{\rho_s^n} e^{-in\theta_s}$$

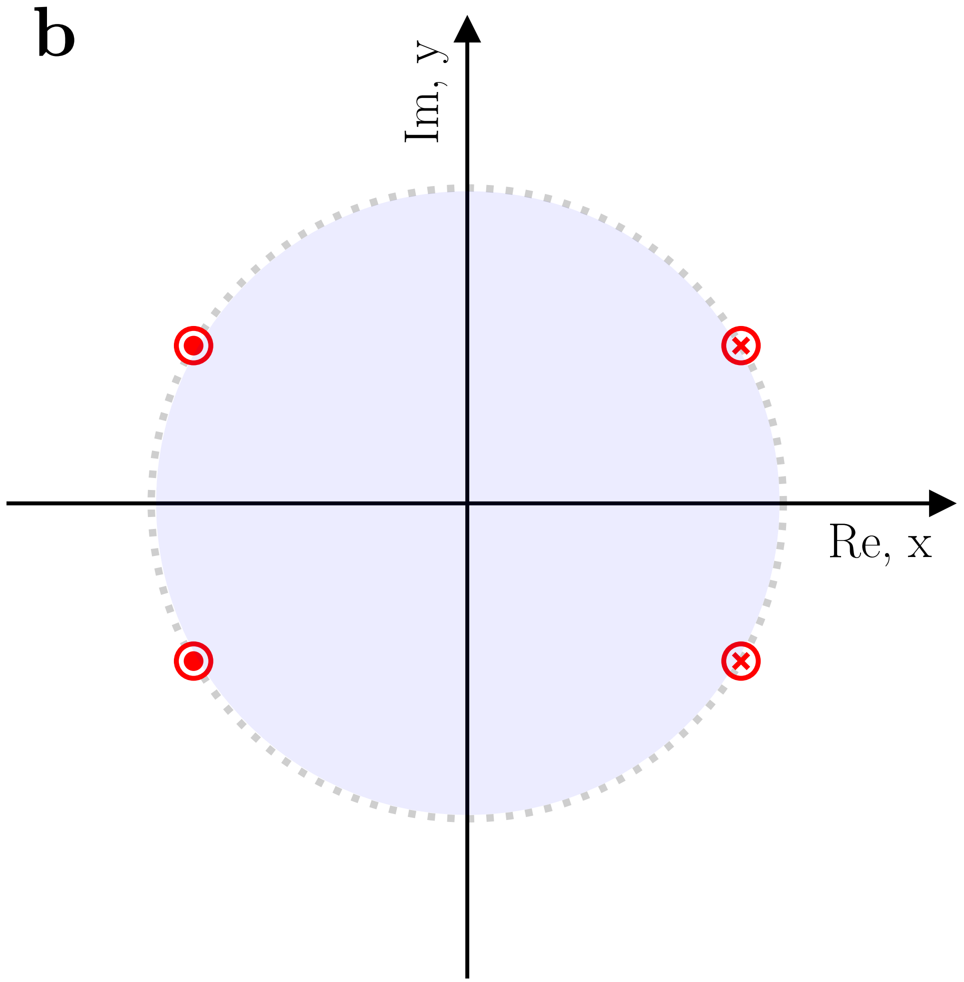

$$\mathbf{B}(z) = \sum_{n=1}^{\infty} C_{n,total} \left(\frac{z}{R_{ref}} \right)^{n-1}$$

$$C_{n,total} = -\frac{\mu_0 R_{ref}^{n-1}}{2\pi} \sum_{j=1}^{m} \frac{I_j}{\rho_j^n} e^{-in\theta_j}$$

$$C_{n,total} = -\frac{\mu_0 I}{2\pi} \frac{R_{ref}^{n-1}}{\rho^n} \sum_{j=1}^{m} s_j e^{-in\theta_j}$$

$$C_{n,q} = \frac{\mu_0 I}{\pi} \frac{R_{ref}^{n-1}}{\rho^n} \cos\left(n\theta_q\right) \left(1 - e^{in\pi}\right)$$